DEVELOPMENT OF AN OCEANIC RAIN ACCUMULATION PRODUCT IN SUPPORT OF SEA SURFACE SALINITY MEASUREMENTS FROM AQUARIUS/SAC-D

by

SHADI ASLEBAGH
B.S. Khaje Nasir Toosi University of Technology, 2005

A thesis submitted in partial fulfillment of the requirements
for the degree of Master of Science
in the Department of Electrical Engineering and Computer Science
in the College of Engineering and Computer Science
at the University of Central Florida
Orlando, Florida

Spring Term
2013

Major Professor: W. Linwood Jones

ABSTRACT

Aquarius/SAC-D is a joint mission by National Aeronautics and Space Administration (NASA) and the Comision Nacional de Actividades Espaciales (CONAE), Argentine Space Agency. The satellite was launched in June 2011 and the prime remote sensing instrument is also named Aquarius (AQ). The main objective of this science program is to provide Sea Surface Salinity (SSS) maps of the global oceans every 7 days for understanding the Earth's hydrologic cycle and for assessing long-term global climate change.

The Aquarius instrument was built jointly by NASA's Goddard Space Flight Center and the Jet Propulsion Laboratory. It is an active/passive L-band remote sensor that measures ocean brightness temperature (Tb) and radar backscatter, and these quantities are used to infer sea surface salinity.

Other environmental parameters (e.g., sea surface temperature, wind speed and rain) also affect the microwave emitted radiance or brightness temperature. The SSS geophysical retrieval algorithm considers all these environmental parameters and makes the Tb corrections before retrieving SSS. Instantaneous rainfall can cause increase roughness that raises the ocean surface Tb. Further short term rain accumulation can produce a fresh water lens that floats on the ocean surface and dilutes the surface salinity.

This thesis presents results of a study to develop an oceanic rain accumulation (RA) product that may be valuable to remote sensing engineers and algorithm developers and Aquarius scientists. The use of this RA product, along with in situ ocean salinity measurements from buoys, may be used to mitigate the effects of rain on the SSS retrieval.

ACKNOWLEDGMENTS

First, I would like to truly thank Prof. W. Linwood Jones for giving me the great opportunity to purse my master's program with him. It has been a great pleasure for me to work under his supervision and I will be grateful to him forever. He has been a wonderful teacher for me and his lessons, both in personal and professional aspects will remain as invaluable assets throughout my life.

My appreciation goes to my committee members, Prof. Parveen F. Wahid and Dr. William N. Junek, for their valuable comments and guidance.

I had the great opportunity to work with the team members at CFRSL and would like to thank each and every one of them for the memorable moments we had together. They have also been great supporters and openly provided their best help at my hard times, for which I am and will remain thankful.

I would like to thank my family. I am so much blessed to have wonderful parents who have given me the love that has been inspiring me every day of my life. I want to thank my lovely sisters, who have been by my side throughout my life, and true friends whenever I needed them. Last but not the least; I thank my husband for the unlimited love and great support he has brought into my life.

TABLE OF CONTENTS

LIST OF FIGURES

LIST OF ACRONYMS/ABBREVIATIONS

AQ: Aquarius

CONAE: Comision Nacional de Actividades Espaciales (Argentine Space Agency)

EIA: Earth Incidence Angle

IFOV: Instantaneous Field Of View

MWR: MicroWave Radiometer

NASA: National Aeronautics and Space Administration

RA: Rain Accumulation

RR: Rain Rate

SSS: Sea Surface Salinity

SST: Sea Surface Temperature

Tb: Brightness Temperature

TRMM: Tropical Rainfall Measuring Mission

CHAPTER 1: INTRODUCTION

Aquarius/SAC-D (AQ/SAC-D) is a joint earth science satellite program by the National Aeronautics and Space Administration (NASA) and the Argentine Space Agency (Comision Nacional de Actividades Espaciales) (CONAE). For the US contribution, NASA served as the mission project manager, developed the prime remote sensor instrument, also named Aquarius (abbreviated as AQ throughout this thesis), and provided the launch from Vandenberg, CA in June 2011. For the Argentine contribution, CONAE provided the satellite platform (known as SAC-D) and several secondary instruments, which support the mission science [1].

The main objective of this mission is to provide the scientists with long term, global scale salinity (the concentration of dissolved salt in sea water) which improves their understanding of the earth's water cycle, ocean circulation and climate [2]. By monitoring seasonal and inter-annual variation of Sea Surface Salinity (SSS), scientists are able to understand ocean circulation and its relationship to climate and the global water cycle [3].

AQ is the first NASA's space-based mission to measure SSS over entire globe and its operational life is three years. It provides monthly global maps of SSS measurements with high spatial (150Km) resolution and a precision of 0.2 practical salinity units (psu) which is equivalent of a pinch (about 1/8 tea spoon) of salt in a gallon of water. This is a

very challenging task, which corresponds to measuring changes in the ocean surface microwave brightness temperature (Tb) to about 0.1 Kelvin [4].

To support this ocean Tb measurement accuracy requirement, several ancillary instruments, including the CONAE MicroWave Radiometer (known as MWR) have been developed and installed on the AQ/SAC-D [5]. They provide Aquarius with additional information about geophysical parameters (e.g. ocean surface wind speed and rainfall) that are used to make corrections in the AQ ocean surface Tb measurements, which results in more accurate SSS retrievals.

1.1 Overview of Aquarius Instrument

The AQ is the prime passive/active microwave remote sensor for measuring SSS. The radiometer (passive instrument) operates at 1.41 GHz and the Tb measurements are used to infer the sea surface salinity. On the other hand, the scatterometer (active instrument) operates at 1.26 GHz, and its role is to provide the L-band radiometer with surface roughness Tb correction in order to remove this (roughness) influence on the retrieval of SSS. A drawing of the AQ/SAC-D observatory is shown in Figure 1.1 [6].

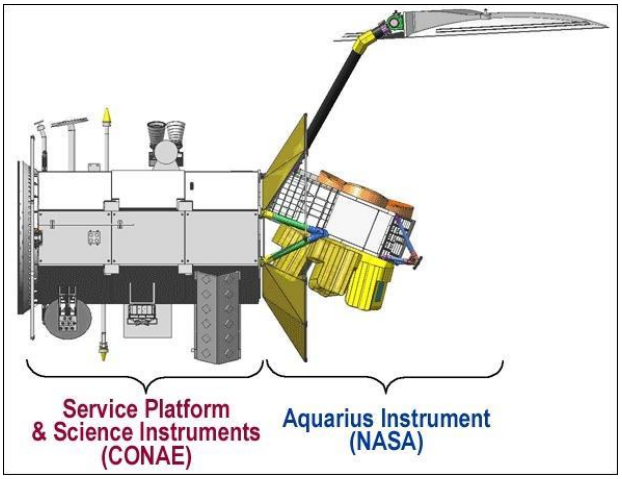

Figure 1.1: Aquarius instrument on the SAC-D satellite bus.

The observatory is an octagonal shaped spacecraft and with the AQ instrument attached. The left-hand part of Fig. 1.1 is the SAC-D service platform where the science instrument provided by CONAE, including MWR, is located and the right-hand side of Fig. 1.1 is the AQ instrument.

1.1.1 AQ/SAC-D Orbit

Aquarius/SAC-D flies in a sun-synchronous polar orbit and crosses over the equator at 6 am (descending) and 6 pm (ascending) local time that is called a terminator orbit. In the terminator orbit, spacecraft follows the sun by flying along the boundary between day and night. The AQ antenna collects energy while looking at the dark side of the earth, which minimizes unwanted solar energy caused by sun glint off the ocean [7].

The orbital parameters have been selected such that the entire extent of ice-free ocean surface between $\pm 80^{o}$ latitude is observed. AQ/SAC-D flies in a circular low earth orbit with an altitude of 657 Km and an inclination of 98^{o}. Being sun synchronous, the orbit

precesses approximately one degree/day, and the orbital ground-track repeats exactly (within a few km) after a period of 103 orbits (~ 7 days) which produces the global SSS maps once a week [7].

1.1.2 AQ Measurement Geometry

The AQ instrument looks to the night side (right hand side) of the satellite sub-track in a push-broom radiometer configuration as shown in figure 1.2 [3]. The antenna has three beams that vary in earth incidence angles (EIA) of 28.7^{o}, 37.8^{o} and 45.6^{o} for inner, middle and outer beams respectively. These instantaneous field of view (IFOV) produce spatial resolutions of 79×94 Km for inner beam, 84×120 Km for middle beam and 96×156 Km for outer beam [8].

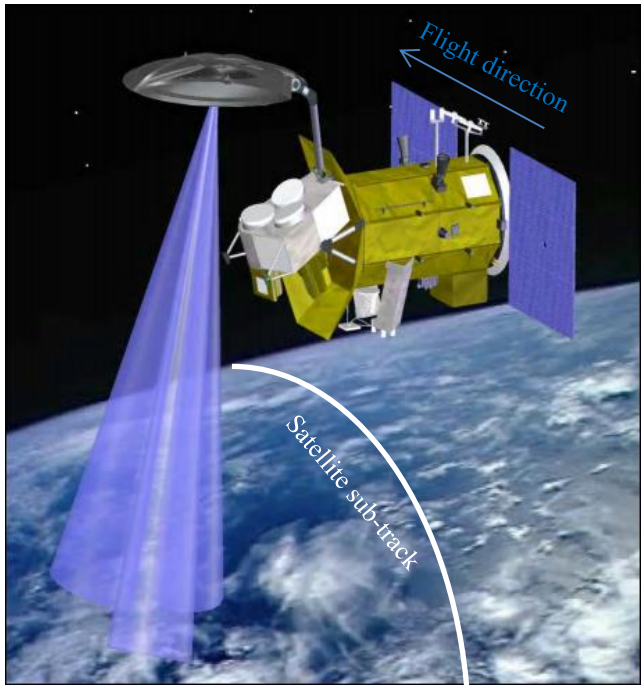

Figure 1.2: Aquarius IFOVs and on-orbit geometry.

Inner and outer beams are slightly aft of the cross track and the middle beam is slightly forward of cross track. An example of the one-day orbital coverage is shown in figure 1.3, where the AQ beam centres are shown as separate orbital tracks. The three beams form the AQ 390 Km measurement swath and during the 7 day period they cover the entire the globe. Afterwards the same orbit ground tracks are repeated every 105 orbits [9].

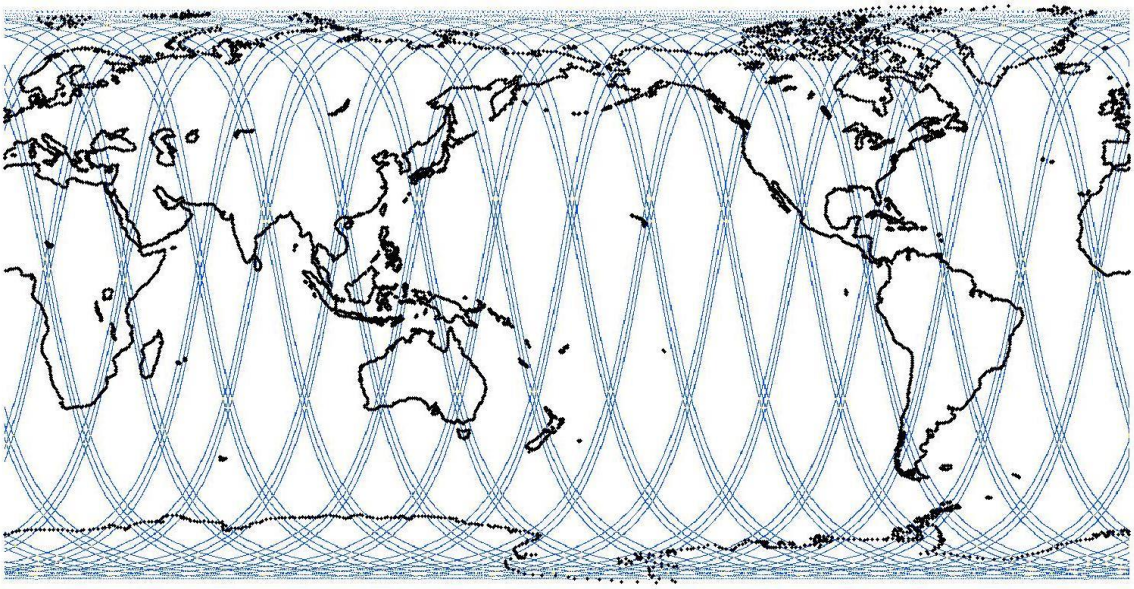

Figure 1.3: Aquarius orbits for one day.

1.1.3 AQ Instrument Description

The AQ antenna is a 2.5 meter offset parabolic reflector with three feed horns as shown in Fig. 1.4. Each feed connects to a separate Dicke radiometer, but the scatterometer is time shared sequentially between horns [10]. Because of the large antenna IFOV, there is

significant overlap between consecutive AQ Tb measurements; therefore, the result is equivalent to simultaneous active/passive L-band measurements, which occur every 1.44 sec.

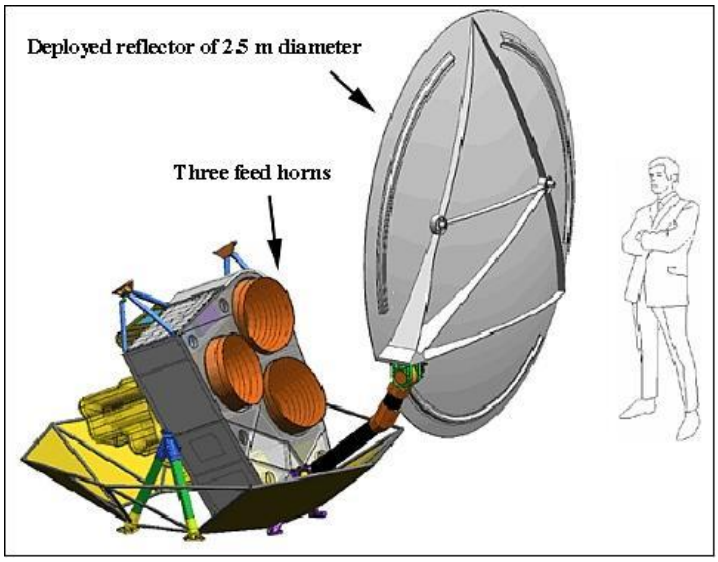

Figure 1.4: Aquarius radiometer main reflector.

To prevent solar contamination, the AQ three horns point away from sun and to the right-hand side and perpendicular to the spacecraft direction of flight. They collect microwave Tb emitted from oceans and send these signals to three Dicke radiometers.

AQ L-band radiometers operate at 1.41 GHz. Being a protected Radio Astronomy band; this is the lowest microwave frequency that can be used for earth observations. More importantly, the ocean Tb at this microwave frequency exhibits high sensitivity to changes in sea surface salinity within the first cm of the ocean depth. Figure 1.5 illustrates how the measured Tb changes with SSS at different sea surface (physical)

temperatures (SST). Each curve corresponds to one specific SSS value, and for a fixed SST, the Tb varies inversely with SSS i.e., increasing SSS decreases the ocean Tb [1].

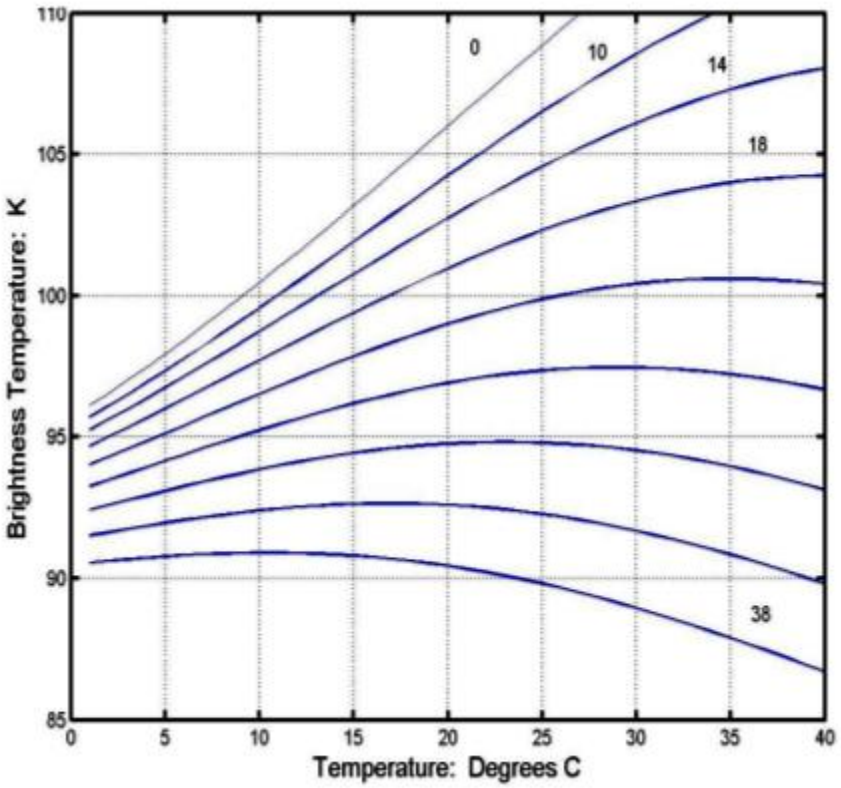

Figure 1.5: Dependence of AQ Tb on SSS and SST.

Further, there are other oceanic geophysical parameters that affect AQ Tb measurements, which must be removed before retrieving the SSS [11]. Of these, ocean surface wind speed is the largest single error source for AQ SSS retrieval. The AQ instrument includes an active microwave scatterometer channel to make simultaneous radar backscatter measurements to correct this roughness error.

Another geophysical parameter that affects the ocean Tb is rain, and it is necessary to study its impact in SSS retrieval algorithm. This is discussed in the following section.

1.2 Rain Impacts on SSS Retrievals

The effects of rain on the measurement of SSS are multifold [12]. First, raindrops striking the ocean increase the surface roughness, which raises the ocean surface Tb and which results in a decrease of the retrieved SSS. Since rain is heterogeneous (transient) in space and time, simultaneous rain measurements during the collection of AQ L-band Tb are highly desirable.

Moreover, over time periods of hours, rain accumulation can produce a fresh water lens that can partially "electromagnetically mask" the ocean salinity [13]. Since fresh water is less dense than the saline water it floats on the salt water and make a layer of fresh water above the sea water. Eventually this fresh water will mix with sea water and dilute the surface salinity. Diffusion of dissolved salt into fresh water and the mechanical mixing of ocean waves eventually restore the ocean surface salinity in time. Thus this is a complicated fluid dynamics process which is driven by the rain accumulation over an AQ IFOV. Unfortunately the repeat period for spatial sampling is 7 days for AQ, which is far too long to resolve this dynamic process. Therefore it is important that other ancillary information on the rain accumulation (integral of rain rate) over each AQ IFOV be provided.

1.3 MWR Instrument Description

To provide this secondary information there is an ancillary instrument on AQ/SAC-D named the CONAE MicroWave Radiometer (MWR) [14]. MWR has three radiometer channels and 8 antenna horns per channel that creates two sets of 8 IFOVs (8 aft-looking and 8 forward-looking of sub-satellite point), which provides several spatially and temporally collocated geophysical parameters that aid in the AQ SSS retrieval. The most important of these parameters are the ocean surface wind speed and rain rate [15, 16].

Concerning the rain rate retrieval, the MWR operates in the K- and Ku-frequency bands (23.8 GHz and 36.5 GHz) that are very sensitive to rain over the oceans. In order to provide AQ with rain rate information, it is important that the measurements be collocated with AQ in space and time. Figure 1.6 shows the overlapping MWR swath with AQ in order to provide near-simultaneous measurements with AQ, where the MWR 8 horn footprints overlap the three AQ IFOVs [5].

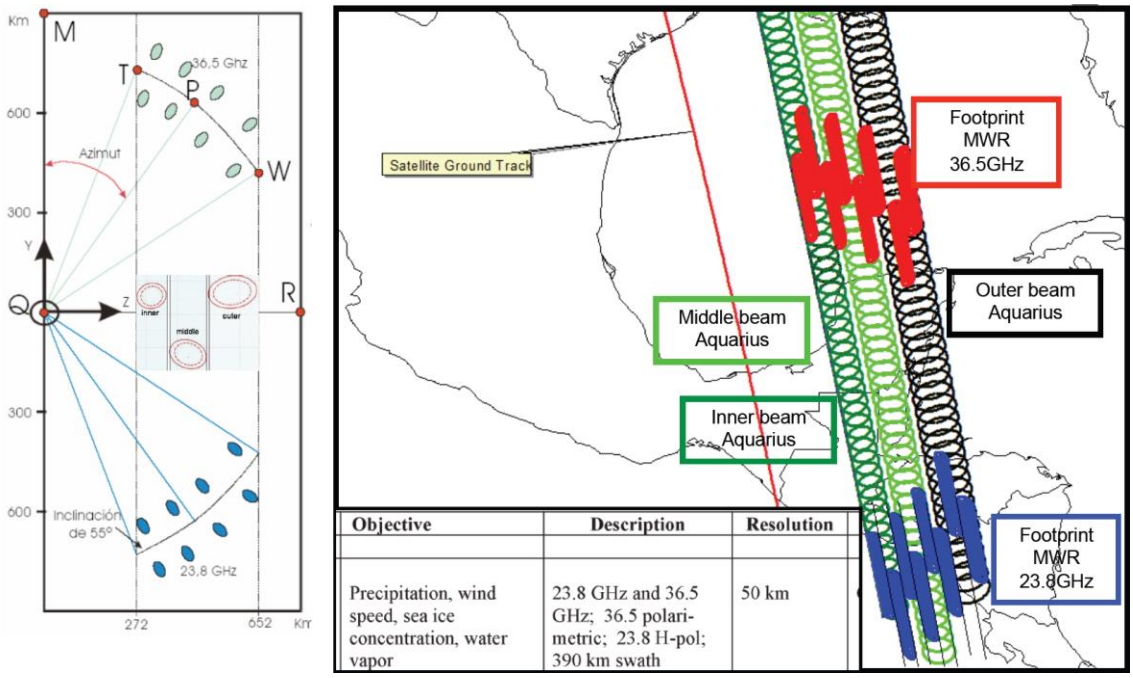

Objective	Description	Resolution
Precipitation, wind speed, sea ice concentration, water vapor	23.8 GHz and 36.5 GHz; 36.5 polari-metric; 23.8 H-pol; 390 km swath	50 km

Figure 1.6: Aquarius and MWR overlapping swath.

The time difference between the MWR forward and aft beams measurements is approximately 4 minutes; so AQ measurements are ± 2 min from the MWR, which is essentially simultaneous over the 100 km AQ IFOV area. Therefore near-simultaneous measurements of environmental parameters such as wind speed and rain rate are provided by MWR over AQ footprint.

As discussed above, in the short term (less than 24 hours) rain accumulation produces a fresh water lens that dilutes the surface salinity. Over time, diffusion of salt into fresh water and mechanical mixing by ocean waves will slightly restore the ocean surface salinity. This process is scientifically important as global salinity patterns are linked to the earth's water cycle of oceanic evaporation and precipitation. More evaporation increases the SSS and precipitation over oceans lowers the SSS.

1.4 TRMM 3B42 Global Rain Product

To develop the AQ rain accumulation product, we used an independent, satellite-derived, ocean rain rate product from the Tropical Rainfall Measuring Mission (TRMM) [17]. We selected the TRMM 3B42 rain rate product, which is near-global rain rate data set that is produced in 3 hour windows. The 3B42 has a $0.25^{o}\times0.25^{o}$ spatial resolution and its spatial coverage extends from $\pm50^{o}$ latitude and $\pm180^{o}$ longitude [18].

The 3B42 rain rate, spatially and temporally collocated with each AQ footprint at the observation time (T_0), was used to calculate the instantaneous rain rate. To calculate the rain accumulation (RA) in 3 hour windows prior to T_o, it is assumed that rain rate varied linearly over the three hour interval between 3B42 snapshots, and the algorithm to calculate RA is described in Chapter 3.

1.5 Thesis Objectives

The objective of this thesis is to develop an AQ rain accumulation product, which enhances the Aquarius Science Team's ability to provide improved calibration and analysis of SSS measurements in the presence of rain. This data product will be a matrix overlay of the AQ L-2 SSS measurements data product provided by NASA. As such it will have a format that is compatible with the L-2 for ease of use.

This auxiliary data set of collocated rain accumulation over the AQ IFOV's can be used for several purposes, namely;

1. as a quality control flag to identify the rain accumulation for the previous 24 hours in 3-hour time steps,
2. to allow SSS retrieval algorithm developers to examine the effects of instantaneous and accumulated rain,
3. to provide an independent estimate of rain accumulation to evaluate the dilution of SSS by rain fall

This thesis is organized in five chapters. Following this introduction, Chapter 2 provides a description of the two different data sets that are used in this thesis. These include; AQ level-2 data and TRMM 3B42 rain rate product. In Chapter 3 the digital processing algorithm to develop the RA product is described. The fourth chapter presents typical algorithm results and anecdotal cases to validate the algorithm and the RA product. Finally in Chapter 5, conclusions are presented and suggestions for future work are given.

CHAPTER 2: DATA DESCRIPTION

This chapter introduces two data sets that are used in this thesis to develop the rain accumulation (RA) product for AQ. The first data set is AQ Level-2 (L-2) science data that is generated from AQ instrument data telemetered from SAC-D. This contains AQ microwave measurements along with date/time stamp and corresponding latitude/longitude (Lat/Lng) coordinates of measurement locations and other auxiliary data [19]. The second data set is TRMM 3B42 which is an independent satellite-derived ocean rain rate product. The 3B42 provides near-global "snapshots" of rain rate every 3-hrs [17], and these rain rates values are utilized to produce RA product over AQ footprints (IFOV's).

2.1 Aquarius L-2 Data

Aquarius L-2 science data product, which is used in this thesis, is version 1.3.1. These archive products are produced and distributed by the NASA Goddard Space Flight Center's Aquarius Data Processing System (NASA/GSFC ADPS), and they are available to the general public through the Physical Oceanography Distributed Active Archive Center (PODAAC) at the NASA Jet Propulsion Laboratory (JPL) [20].

Each L-2 file contains data from one orbit that is defined as starting (and ending) when the AQ/SAC-D spacecraft passes South Pole. A plot for one L-2 file is shown in Fig. 2.1, where the ascending pass starts from the bottom right of the figure over Antarctica and

continues to its northern most latitude over the Arctic Ocean. After this point the spacecraft begins the descend pass moving southward until it reaches Antarctica. Note the earth has rotated toward the east during the orbit period so that the starting point of the next orbit moves westward.

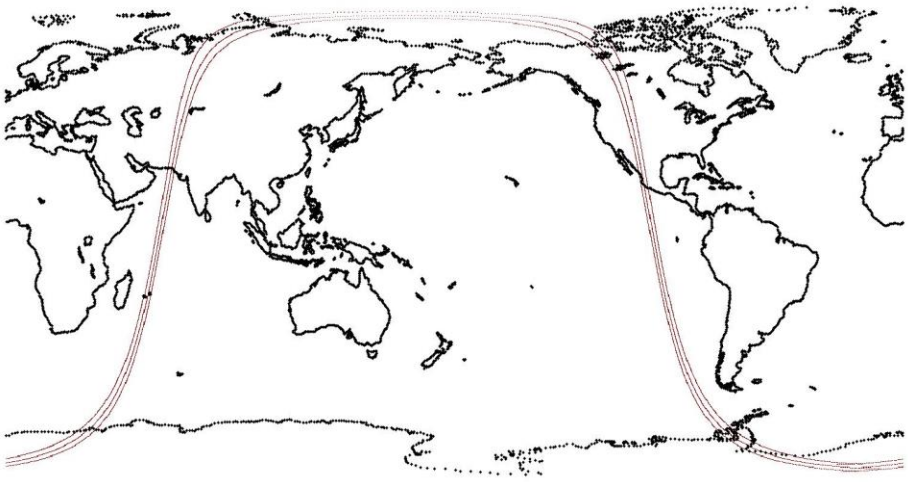

Figure 2.1: An Aquarius orbit corresponding to one AQ L-2 file.

The L-2 data is a time-ordered matrix of data vectors, which occur every 1.44 sec. The data vectors contain: observation data such as: orbit#, date/time tags, measured brightness temperatures (3 beams), radar backscatter (3 beams), satellite sub-point navigation data, satellite attitude (roll, pitch and yaw) and orbit ephemeris. The data vector also contains calculated data such as: AQ cycle#, AQ beam earth incidence and azimuth angles, beam IFOV contour and center locations (Lat/Lng). Finally, the data vectors contain geophysical data from models, auxiliary data bases and the derive AQ science

measurements. The composite of 103 orbits (L-2 files) comprise one AQ cycle, which is the orbit repeat period that provides global coverage [19].

For this thesis, the following L-2 information is used:

1. AQ/SAC-D orbit#: sequential starting at launch in June 11, 2011
2. AQ/SAC-D cycle#: Every 103 AQ orbits comprises one AQ cycle which is approximately one week duration. AQ cycle number (cycle#) is sequential from the AQ instrument turn-on in August 2011.
3. AQ IFOV center location (Lat/Lng) – given by AQ beams (3)
4. AQ observation time – day of year and GMT at the end of the AQ measurement time (1.44 sec)
5. AQ flags – "surface classification" flags to identify observations over ocean, land, ice and mixed and data quality flags.

2.2 TRMM 3B42

The rain rate values used in this thesis are provided by TRMM 3B42 product. The Tropical Rainfall Measuring Mission (TRMM) is a NASA LEO (Low Earth Orbit) satellite designed to measure rain fall in the tropics. The TRMM 3B42 rain product is a near-global, earth gridded ($0.25^{o}\times0.25^{o}$ latitude/longitude) composite rain image of all available rain estimates that occur within a 3-hour window (eight 3B42 rain images/day) [17].

These rain estimates, provided by both microwave and InfraRed (IR) remote sensors on multiple cooperative satellites, are blended to form near-global (50^o south to 50^o north latitude) rain image. The image is formed from all satellite rain estimates available within a 3-hr window centered on: 00, 03, 06, 09, 12, 15, 18 and 21 hours Greenwich Median Time (GMT). Because the rain estimates from microwave sensors are superior to those provided by IR, when microwave are available, they are used. The algorithm used for production of 3B42 is explained below.

First, the microwave estimates of precipitation from the various satellites are cross calibrated relative to TRMM Precipitation Radar and TRMM Microwave Imager (TMI) satellite rain retrievals. This cross calibration to TRMM ensures a consistent, high quality rain rate product that is independent of the observing instrument. Afterwards, these rain rate observations are combined to produce a global rainfall image [21, 22]. When multiple microwave satellite observations overlap spatially, then a weighted average is calculated.

A typical 3B42 rain rate image for only the microwave radiometer measurements is shown in figure 2.2. Light blue color shows the swaths of the microwave radiometers, and the white color shows regions where no microwave measurements are available. The x-axis is longitude (±180°) and y-axis is latitude (±50°) and each rain rate image has a spatial resolution of $0.25^o \times 0.25^o$, so each file is a matrix size of 400×1440. In this figure, rain rate in mm/hr is shown in color, and note that rain occurs over both land and oceans; however, for this thesis, we are only concerned with ocean rain rates.

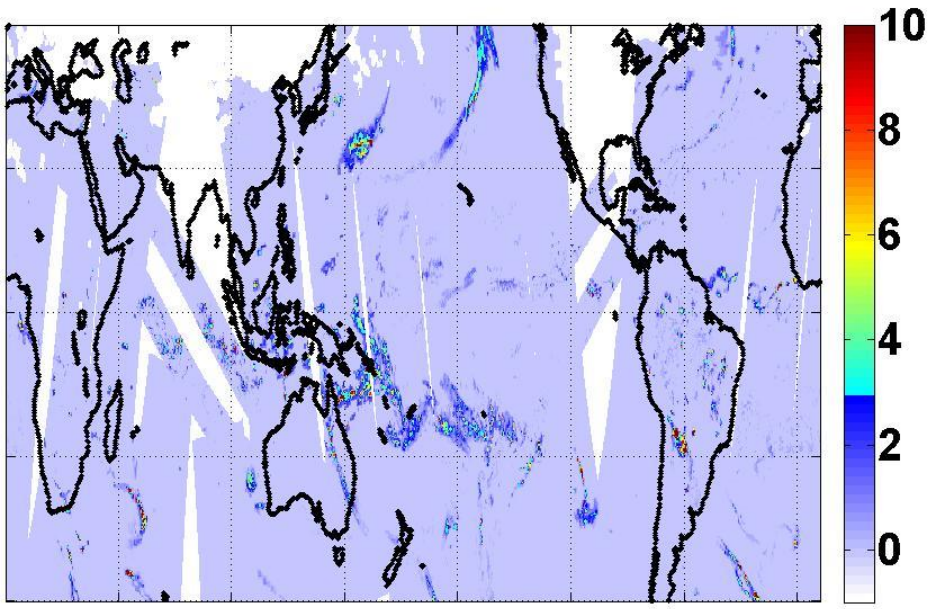

Figure 2.2: Typical 3B42 rain image using only microwave radiometer measurements.

After creating the composite microwave rain image, the next step is to include the IR precipitation estimates, which are also cross calibrated to TRMM. Thus, the IR are blended to fill-in the gaps between microwave radiometer swaths [22]. Further, in addition to the rain rate information, there is another field in the 3B42 product that contains a corresponding quality flag that specifies which source (microwave or IR) was used.

An example of eight 3B42 rain rate images is shown in Fig. 2.3, where the rain rate in mm/hr is shown in color. Figure 2.4 also shows the zoomed-in view of one rain event (shows in red circles in Fig. 2.3) for the same 3B42.

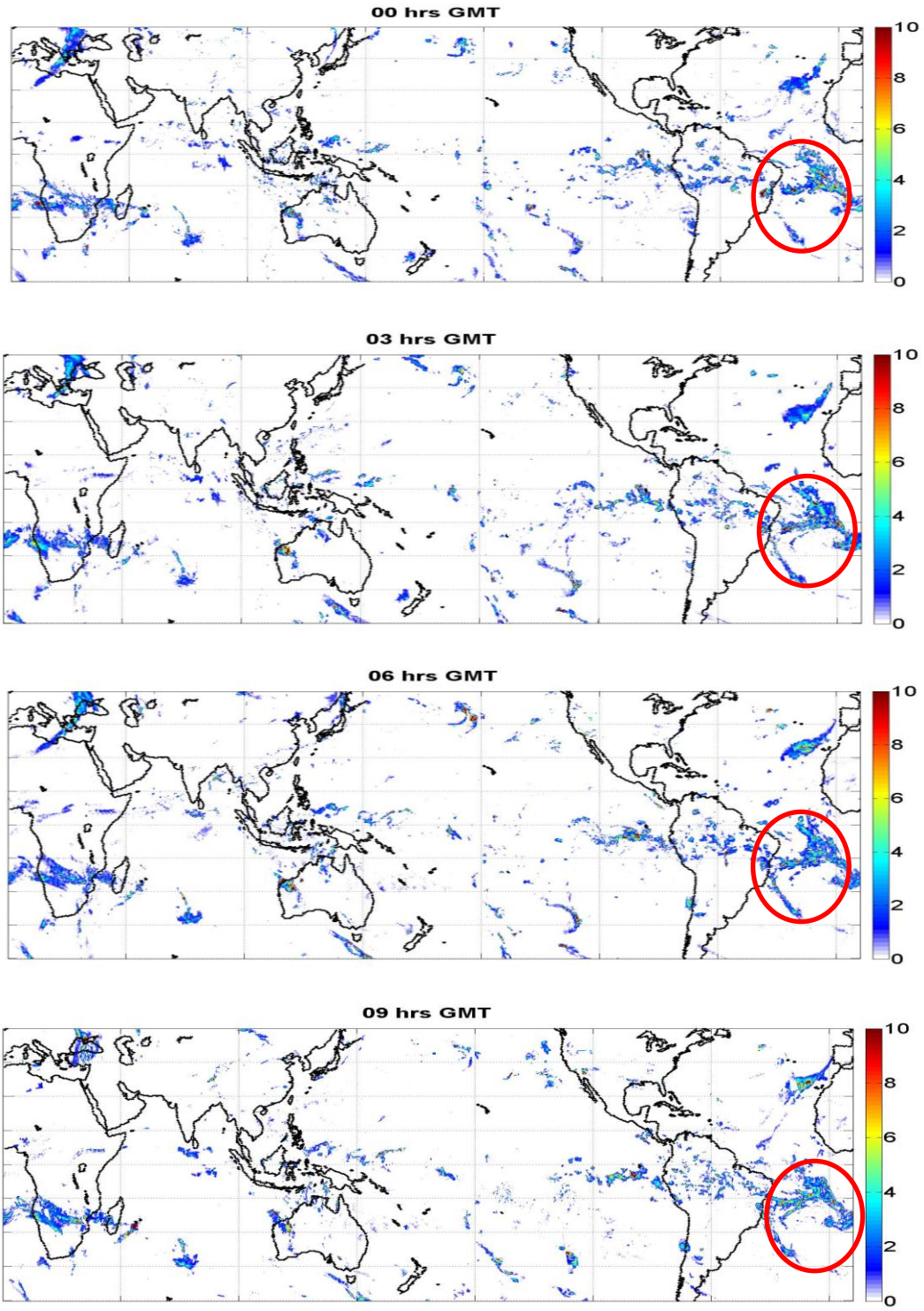
00 hrs GMT
03 hrs GMT
06 hrs GMT
09 hrs GMT
10
8
6
4
2
0

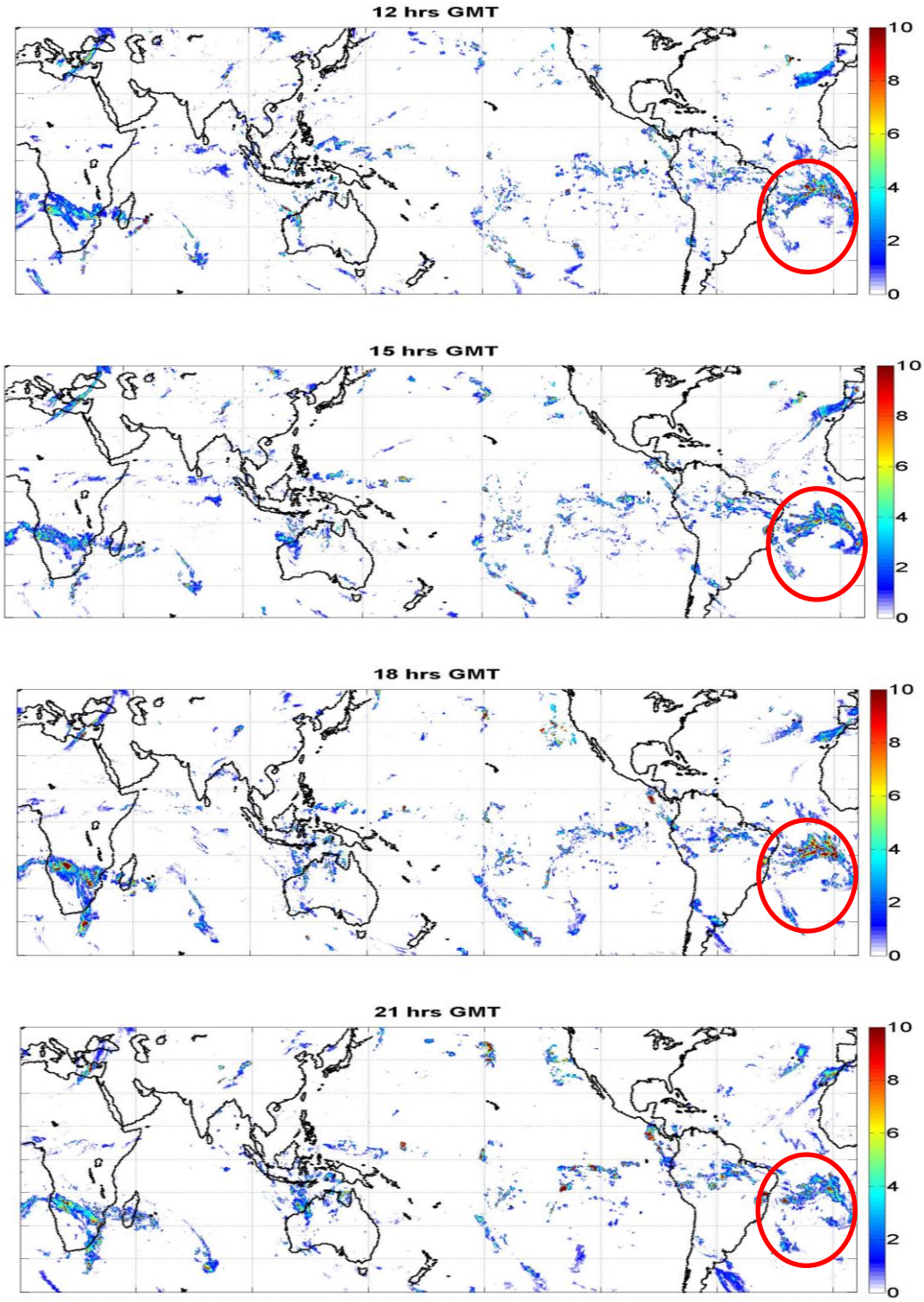

Figure 2.3: Rain rate images for one 3B42 file for 00, 03, 06, 09, 12, 15, 18 & 21 hrs GMT.

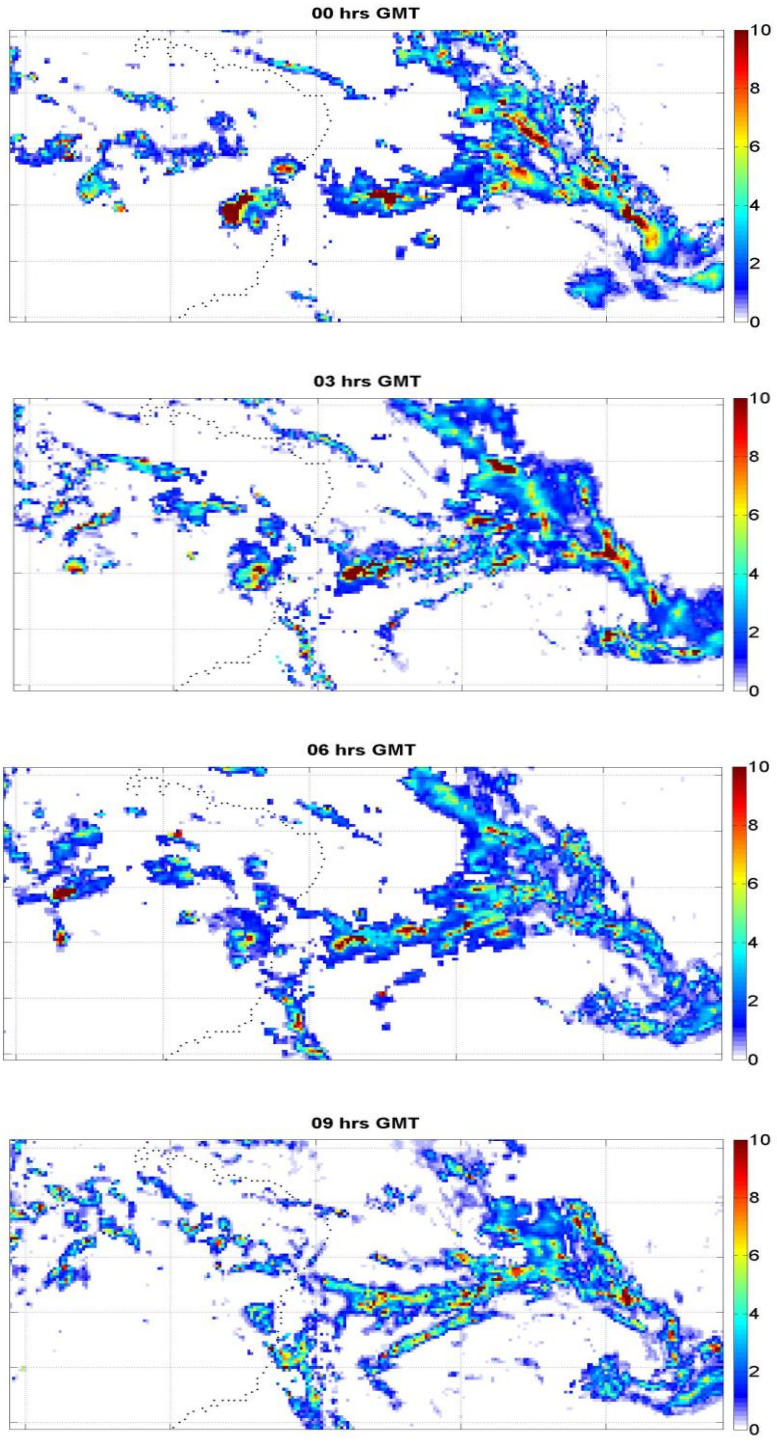
00 hrs GMT
03 hrs GMT
06 hrs GMT
09 hrs GMT
10
8
6
4
2
0

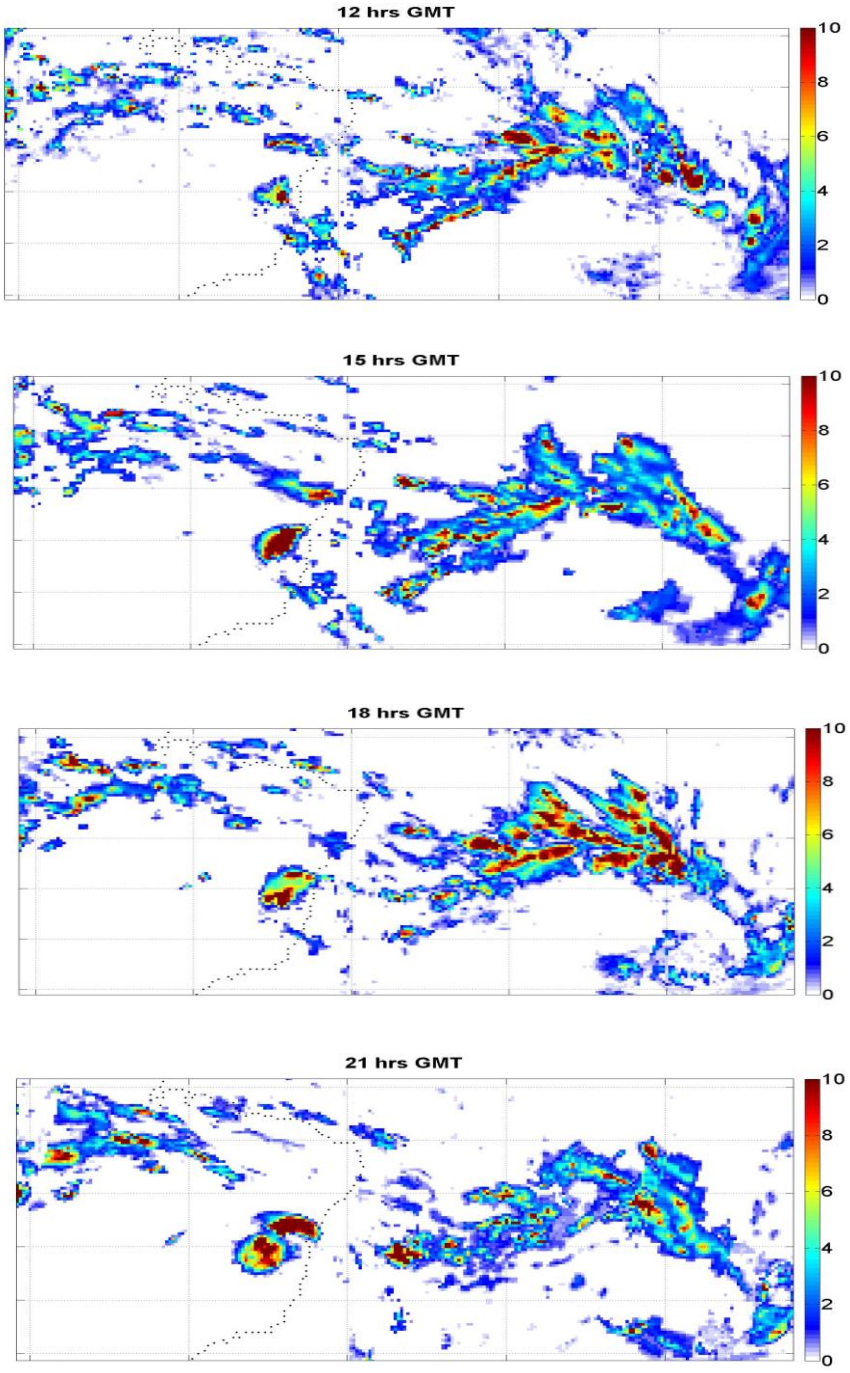

Figure 2.4: Zoomed-in view of one rain event for one 3B42 file for 00, 03, 06, 09, 12, 15, 18 & 21 hrs GMT.

A review of this time series of 3B42 images shows that rain heterogeneous in space and time. Over the global scale, there appears to be significant correlation between rain images; however, at the AQ IFOV scales (~100km), there is considerable variability between 3B42 images. For our purposes of creating an AQ RA product, a 1-hr temporal sampling of the global rain field is desirable, but this is not presently available. In the future, this will be provided by NASA Global Precipitation Mission to be launched in 2016, which comprises a constellation of rain measuring satellites [23]. Therefore, in developing the RA product, it is necessary to perform a high temporal-interpolation (every 15 minutes) over a 24 hr period. We assume that the rain rate at a given pixel varies linearly in time between the 3B42 snapshots. This may not be true, but it is a matter of necessity because the actual rainfall temporal variation is unknown.

3B42 data are accessed via NASA Goddard Earth Sciences Data and Information Services Center (GES DISC) and they are accessible by using Mirador at GES DISC. The 3B42 products used in this thesis are in version 7 [24].

CHAPTER 3: RAIN ACCUMULATION ALGORITHM

This section describes the algorithm for producing an AQ rain accumulation product that will be an overlay for the AQ L-2 SSS science data. This means that each AQ observation (row of the file) contains the instantaneous rain rate (RR) and the rain accumulation (RA) in eight 3-hour windows for the previous 24 hours.

3.1 RR/RA Algorithm Architecture

The architecture of the RR/RA algorithm is illustrated in the flow diagram of Fig. 3.1.

The algorithm inputs are earth gridded ($0.25^{o}\times0.25^{o}$) files for both AQ and 3B42 data. The output of this digital processing algorithm is the earth gridded instantaneous rain rate and the rain accumulation over the three AQ beam IFOV's for the time windows: 3, 6, 9, 12, 15, 18, 21 and 24 hours prior to AQ observation time.

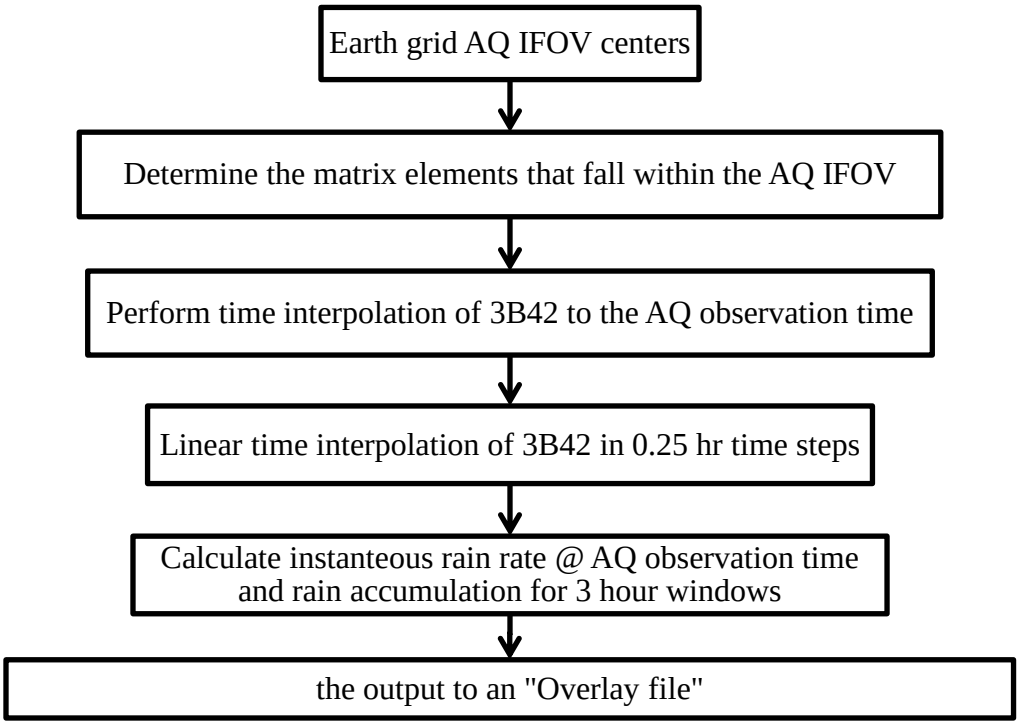

Figure 3.1: RR/RA algorithm flowchart.

3.2 RR/RA Algorithm Description

The first step in this algorithm is to earth grid AQ IFOV centers and determine the corresponding AQ observation time. Next, we determine the matrix (earth grid) elements that fall within the AQ IFOV, which is illustrated in Fig. 3.2. The red circle represents the AQ IFOV, which we approximate as a 100 km diameter circle for each beam. The 13 blue squares represent the earth grid ($0.25^{o}\times0.25^{o}$ boxes) that we select to calculate the RR and RA. The red shaded box contains the center of the AQ IFOV.

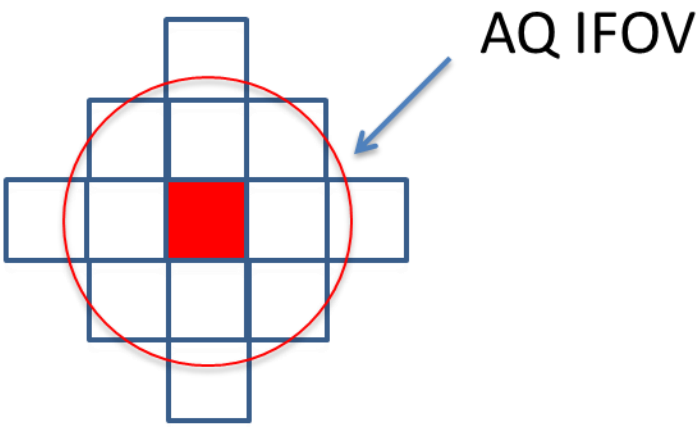

Figure 3.2: Spatial model used to calculate average rain rate and rain accumulation over an AQ footprint.

Using the AQ observation time (T_o), we linearly interpolate the two 3B42 rain rate, which bracket the AQ observation time. Using a 0.25 hr sampling interval, we select the closet sample to be the "instantaneous" rain rate value. Next we select the corresponding 13 IFOV pixels and perform an average (including zero rain rates). This is defined as the "instantaneous rain rate" averaged over the AQ IFOV and it is calculated using equation 3-1.

$$instataneous\ rain\ rate = \left(RR_{a-2,b} + RR_{a-1,b-1} + RR_{a-1,b} + RR_{a-1,b+1} + RR_{a,b-2} + RR_{a,b-1} + RR_{a,b} + RR_{a,b+1} + RR_{a,b+2} + RR_{a+1,b-1} + RR_{a+1,b} + RR_{a+1,b+1} + RR_{a+2,b}\right)/\ 13 \quad (3\text{-}1)$$

Where "a" and "b" are the indices of the pixel corresponding to the centre of the IFOV (red box in Fig. 3.2) and the subscripts denote the matrix indices of the 13 pixels. It should be noted that pixels containing "bogus" rain rates are converted to "NOT A

Number, NAN". In this event that the denominator in Eq. 3-1 will be (13 - #NAN's) because NAN's are not included in the mean calculation.

Next, we repeat this process to calculate the corresponding rain rate for the same 13 pixels for the previous 24 hours in 0.25 hour steps. Finally these are added in 3 hours windows to find the corresponding RA over the AQ IFOV. The final output contains: instantaneous RR and RA for 0-3hr, 0-6hr, 0-9hr, 0-12hr, 0-15hr, 0-18hr, 0-21hr and 0-24hr prior to the AQ observation time.

3.3 Example RR/RA Calculations for one cell

As discussed in Chapter 2, the 3B42 rain rates are available every 3-hr. Figure 3.3 shows 3B42 rain rate for one 0.25°×0.25° pixel within an AQ footprint.

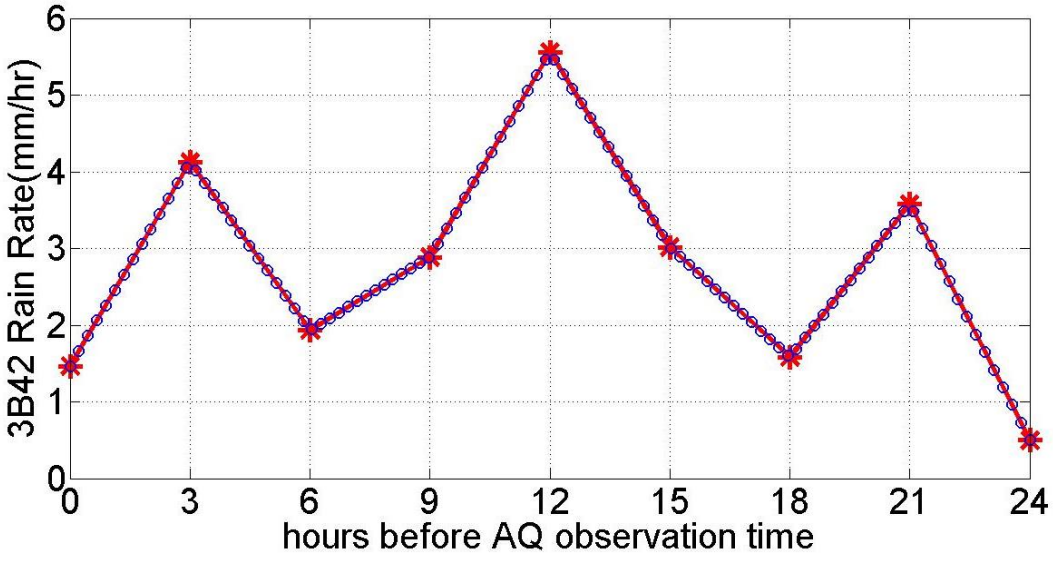

Figure 3.3: Interpolated 3B42 rain rate every 15 minutes.

Figure 3.3 presents original 3B42 rain rate every 3-hr (red asterisk) and also interpolated rain rates every 15 minutes (blue circles). To make the RA more reliable, it is desirable to temporally sample the rain rate in less than 3-hr periods. To achieve this, a linear interpolation is applied to 3B42 rain rate every 15 minutes. As a result instantaneous rain rates are available over AQ footprint every 0.25-hr to calculate the RA.

To calculate RA for previous 3, 6, 9, 12, 15, 18, 21 and 24-hr over each cell a set of formulas are introduced in Eq. (3-2) – (3-9).

$$RA_{03} = (RR_{01} \times 0.25) + (RR_{02} \times 0.25) + \cdots + (RR_{12} \times 0.25) \quad (3\text{-}2)$$

$$RA_{06} = (RR_{01} \times 0.25) + (RR_{02} \times 0.25) + \cdots + (RR_{24} \times 0.25) \quad (3\text{-}3)$$

$$RA_{09} = (RR_{01} \times 0.25) + (RR_{02} \times 0.25) + \cdots + (RR_{36} \times 0.25) \quad (3\text{-}4)$$

$$RA_{12} = (RR_{01} \times 0.25) + (RR_{02} \times 0.25) + \cdots + (RR_{48} \times 0.25) \quad (3\text{-}5)$$

$$RA_{15} = (RR_{01} \times 0.25) + (RR_{02} \times 0.25) + \cdots + (RR_{60} \times 0.25) \quad (3\text{-}6)$$

$$RA_{18} = (RR_{01} \times 0.25) + (RR_{02} \times 0.25) + \cdots + (RR_{72} \times 0.25) \quad (3\text{-}7)$$

$$RA_{21} = (RR_{01} \times 0.25) + (RR_{02} \times 0.25) + \cdots + (RR_{84} \times 0.25) \quad (3\text{-}8)$$

$$RA_{24} = (RR_{01} \times 0.25) + (RR_{02} \times 0.25) + \cdots + (RR_{96} \times 0.25) \quad (3\text{-}9)$$

Where RR_i is the interpolated 3B42 rain rate at time $T_o - (i \times 0.25\text{hr})$.

Figure 3.4 shows the 3B42 RA over one AQ cell for the 24hr previous AQ observation time for the same cell in semi-log plot. X-axis is the hours before AQ observation time and Y-axis is the accumulated rain rate in logarithmic scale.

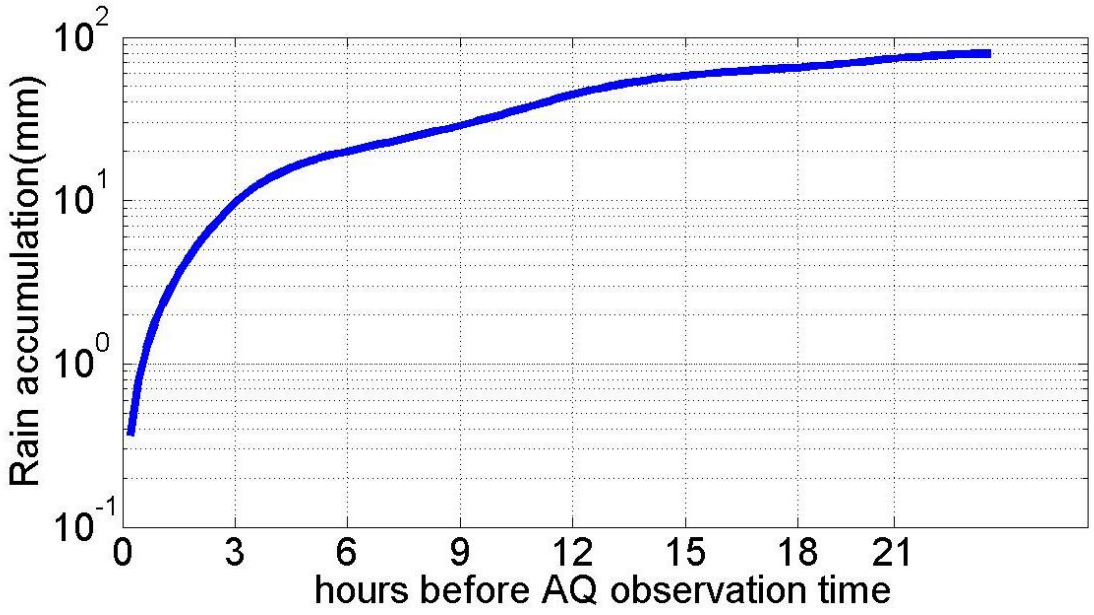

Figure 3.4: 3B42 rain accumulation over one AQ cell.

CHAPTER 4: RESULTS AND VALIDATION

In this chapter examples of RR/RA product are presented, and the validation procedure is discussed.

4.1 RR/RA Results

In this section examples of RA product are presented for one AQ orbit and also one month of AQ orbits.

4.1.1 One AQ Orbit

Since the RA product is intended for comparison with AQ SSS measurements, only "over oceans" data are desired; therefore, it is necessary to exclude land and ice observations using the "surface classification" flags provided in the AQ L-2 science data product. For these pixels the RA is assigned as not-a-number (NAN). Afterwards The RA is calculated using the above described algorithm using equations (3-2) - (3-9) and written into the RA output file for a single AQ/SAC-D orbit. Figure 4.1 shows the 3B42 instantaneous rain rate (mm/hr) at AQ observation time and differential RA (mm) for previous 3 (0-3), 6 (3-6), 9 (6-9), 12 (9-12), 15 (12-15), 18 (15-18), 21 (18-21) and 24 (21-24) hours. The left column shows the ascending part of the AQ orbit and the right column shows the descending part of the orbit. The x-axis is longitude and it is zoomed in for 150-200^{o} longitude for ascending part of the AQ orbit and 300-350^{o} longitude for descending part of the orbit. The y-axis is latitude and it covers ±50^{o}.

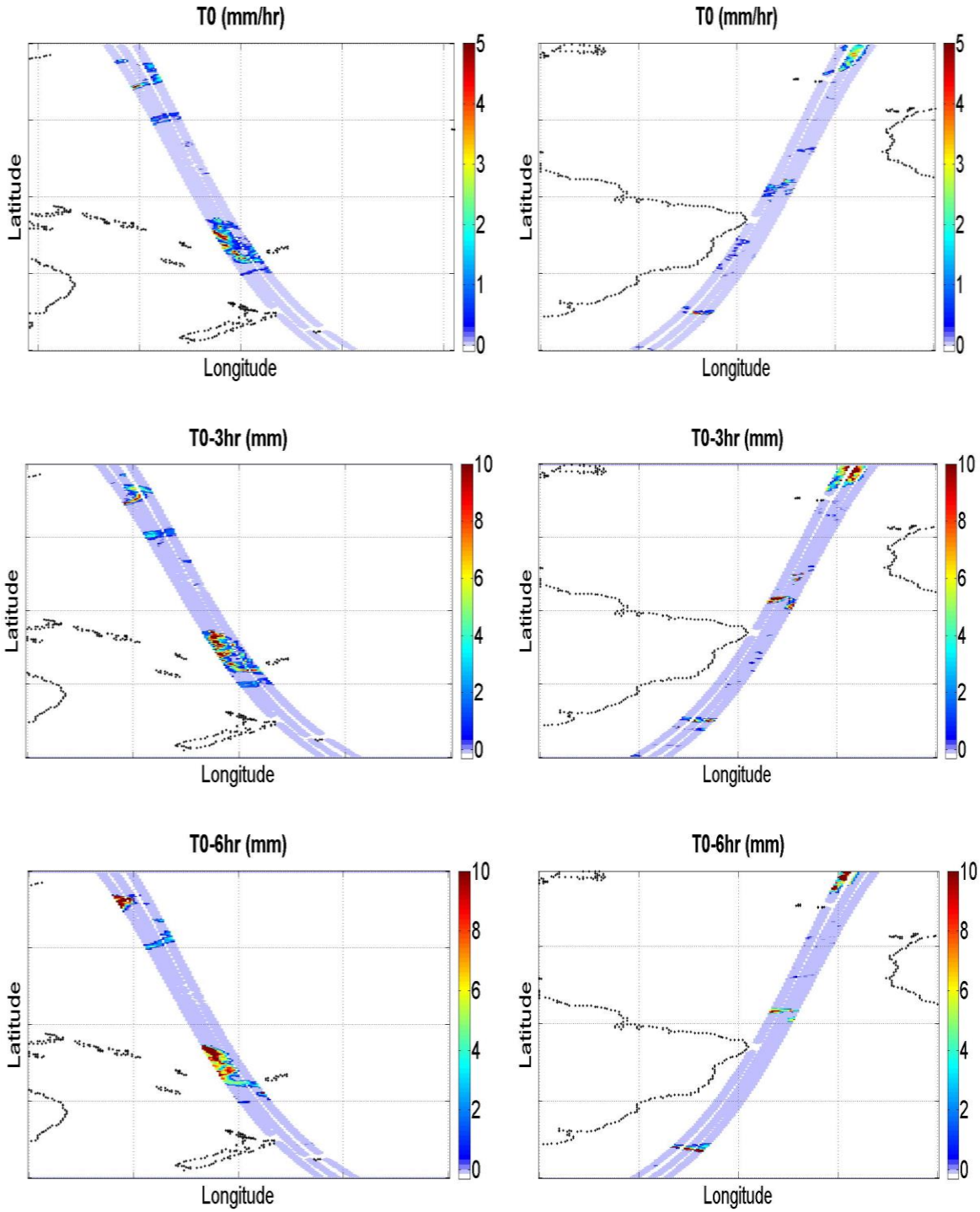
T0 (mm/hr)
Latitude
Longitude
0
1
2
3
4
5
T0 (mm/hr)
Latitude
Longitude
0
1
2
3
4
5
T0-3hr (mm)
Latitude
Longitude
0
2
4
6
8
10
T0-3hr (mm)
Latitude
Longitude
0
2
4
6
8
10
T0-6hr (mm)
Latitude
Longitude
0
2
4
6
8
10
T0-6hr (mm)
Latitude
Longitude
0
2
4
6
8
10

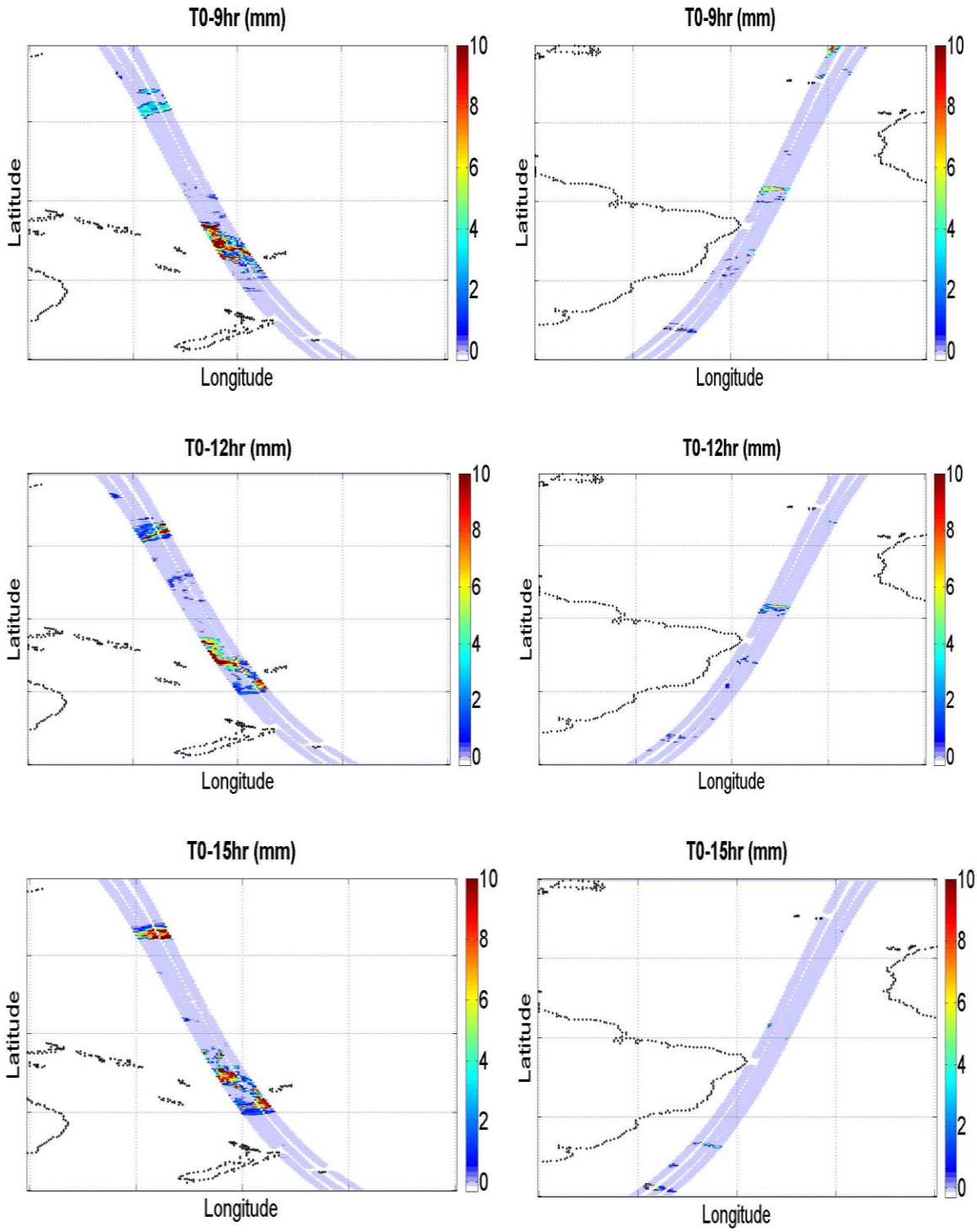
T0-9hr (mm)
T0-9hr (mm)
T0-12hr (mm)
T0-12hr (mm)
T0-15hr (mm)
T0-15hr (mm)
Latitude
Longitude
0
2
4
6
8
10

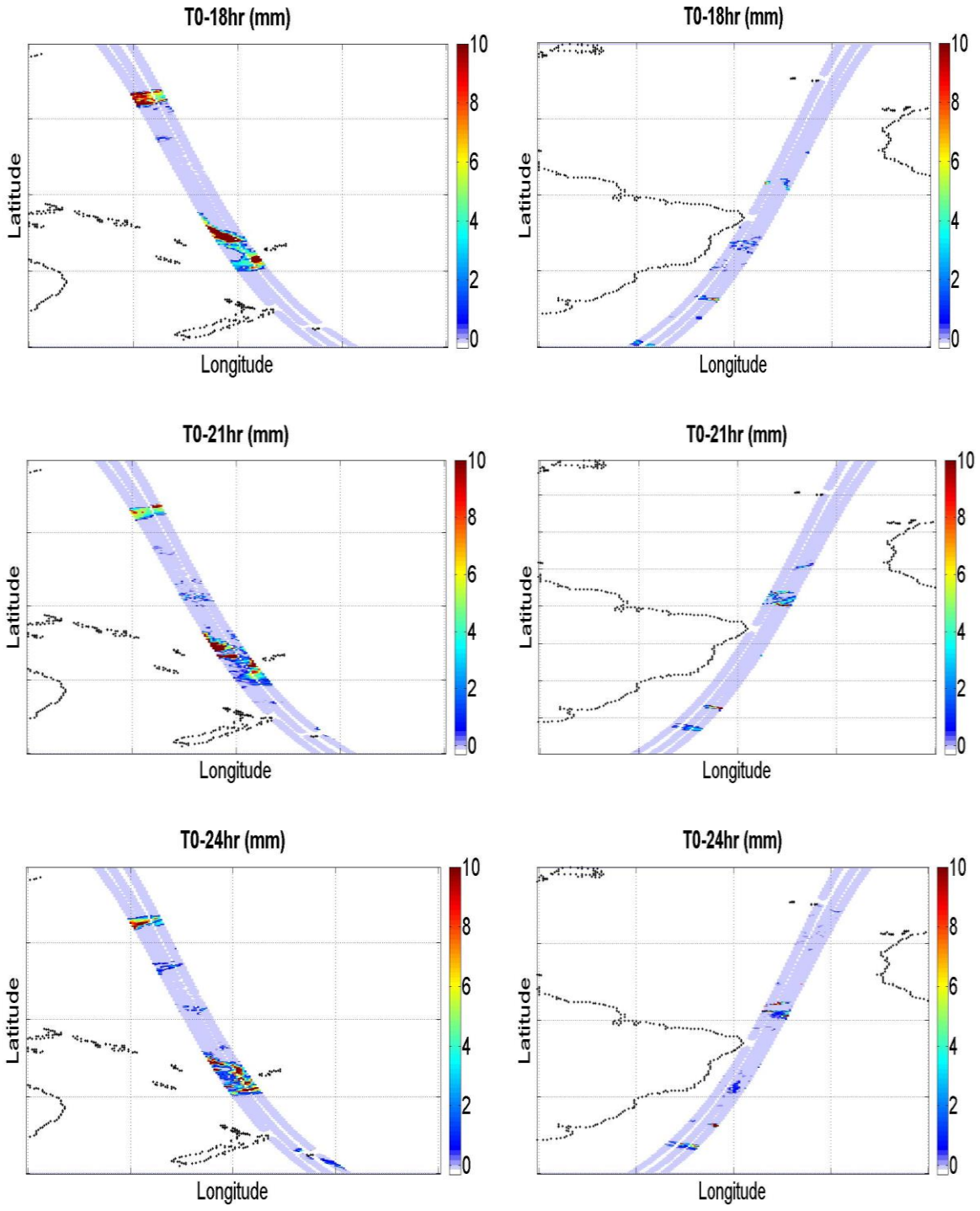

Figure 4.1: Instantaneous 3B42 rain rate and differential RA for one AQ orbit.

Besides, the Rain Accumulation (RA) image, for the previous 6hr period to the AQ observation time and for one AQ/SAC-D orbit, is presented in Fig. 4.2.

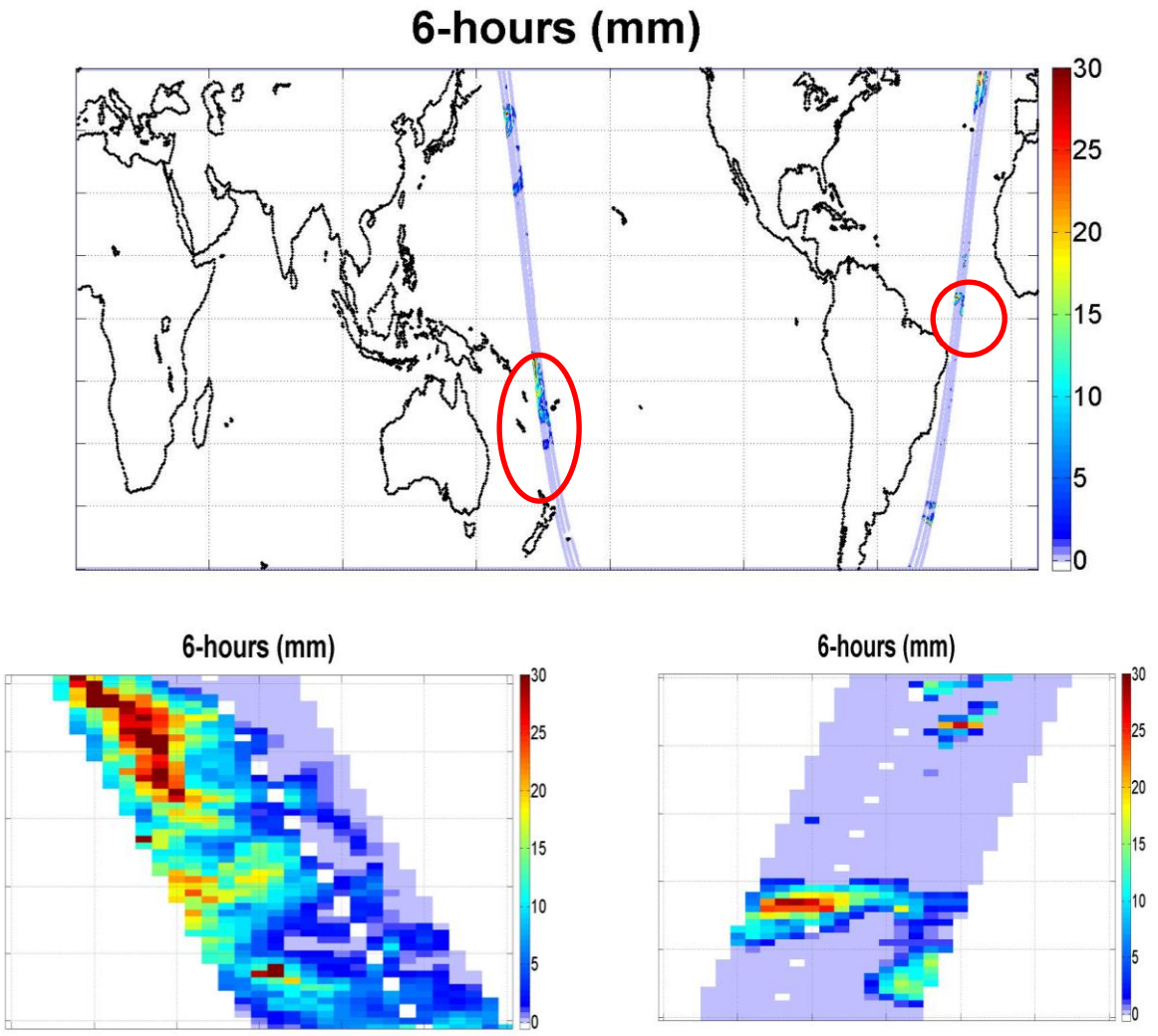

Figure 4.2: RA for 6hr prior to AQ observation time for one AQ orbit.

The image pixels are plotted in color corresponding to the RA in mm. The bottom panel of the figure shows a zoomed-in view of the RA over ascending and descending parts of the AQ/SAC-D orbit. X-axis and Y-axis are longitude and latitude respectively and light blue color shows AQ swath (zero rain rate).

4.1.2 One-month AQ Orbits

The 3B42 instantaneous rain rate interpolated to the AQ observation time is presented in Fig. 4.3 for one month of AQ orbits. It is noted that for each day, nine 3B42 files (8 per day and one from the past day) were used to provide the interpolated instantaneous rain rates at the AQ beam locations.

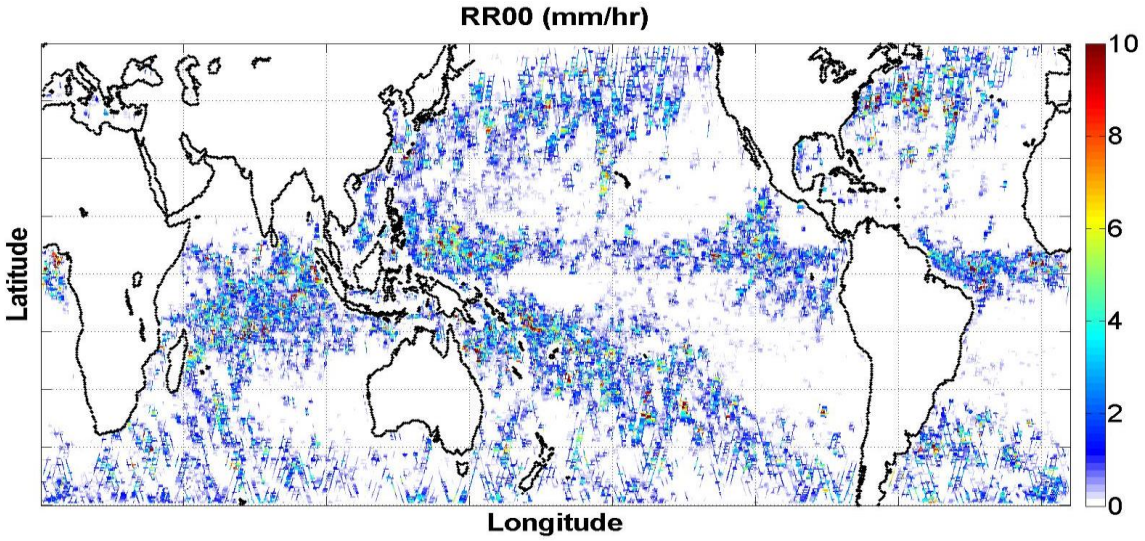

Figure 4.3: AQ instantaneous rain rates (from interpolated 3B42 rain rate) at AQ observation time.

The RA images for one month of AQ orbits are presented in Figs 4.4 for time intervals of T_o-6hr, T_o -12hr, T_o -18hr and T_o -24hr prior to AQ observation time respectively. In these set of figures, color represents the RA in mm.

Figure 4.5 also presents the zoomed-in view of one rain event shown in red circles in Fig. 4.4.

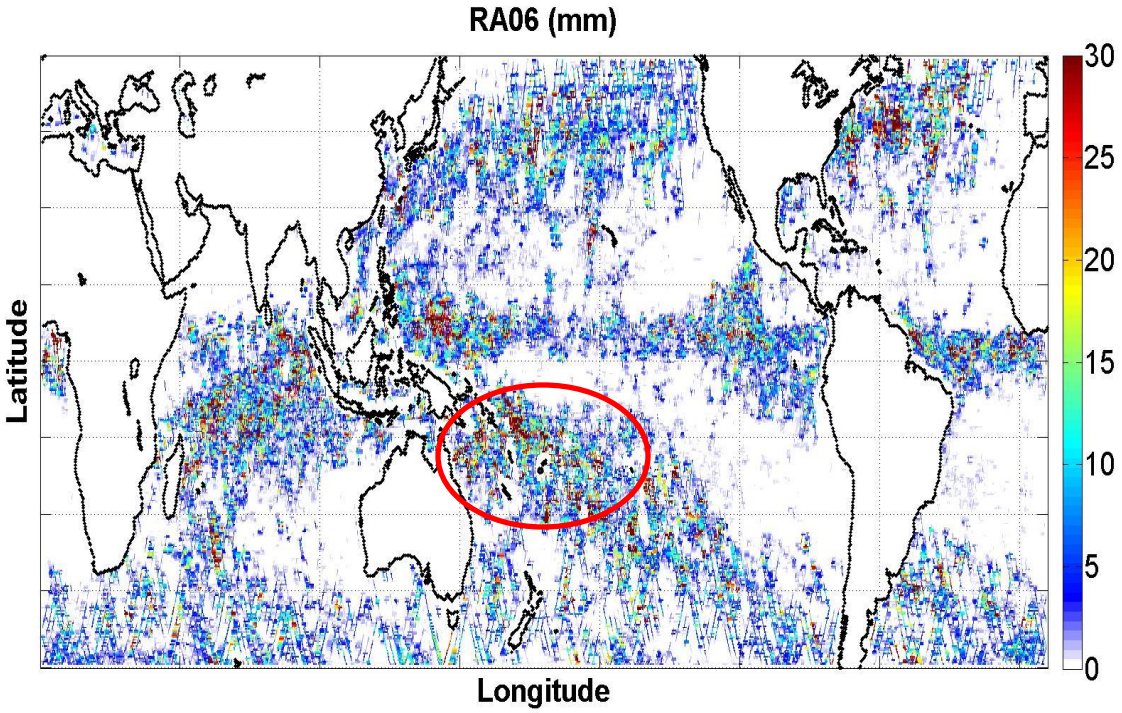
RA06 (mm)
Latitude
Longitude
30
25
20
15
10
5
0

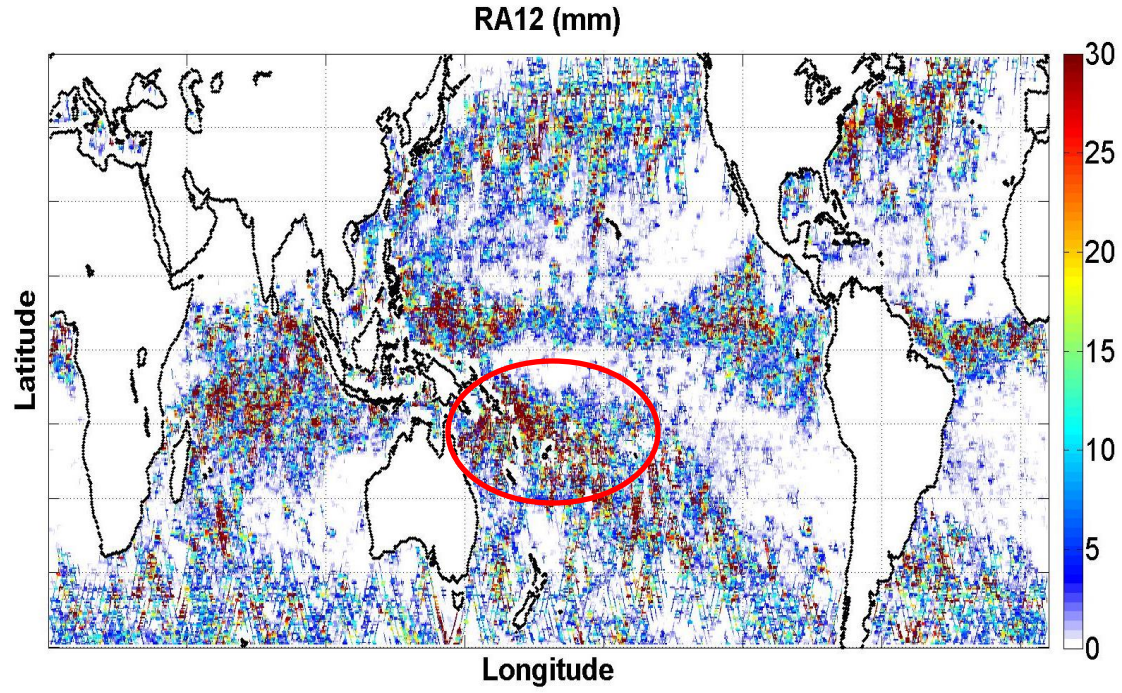
RA12 (mm)
Latitude
Longitude
30
25
20
15
10
5
0

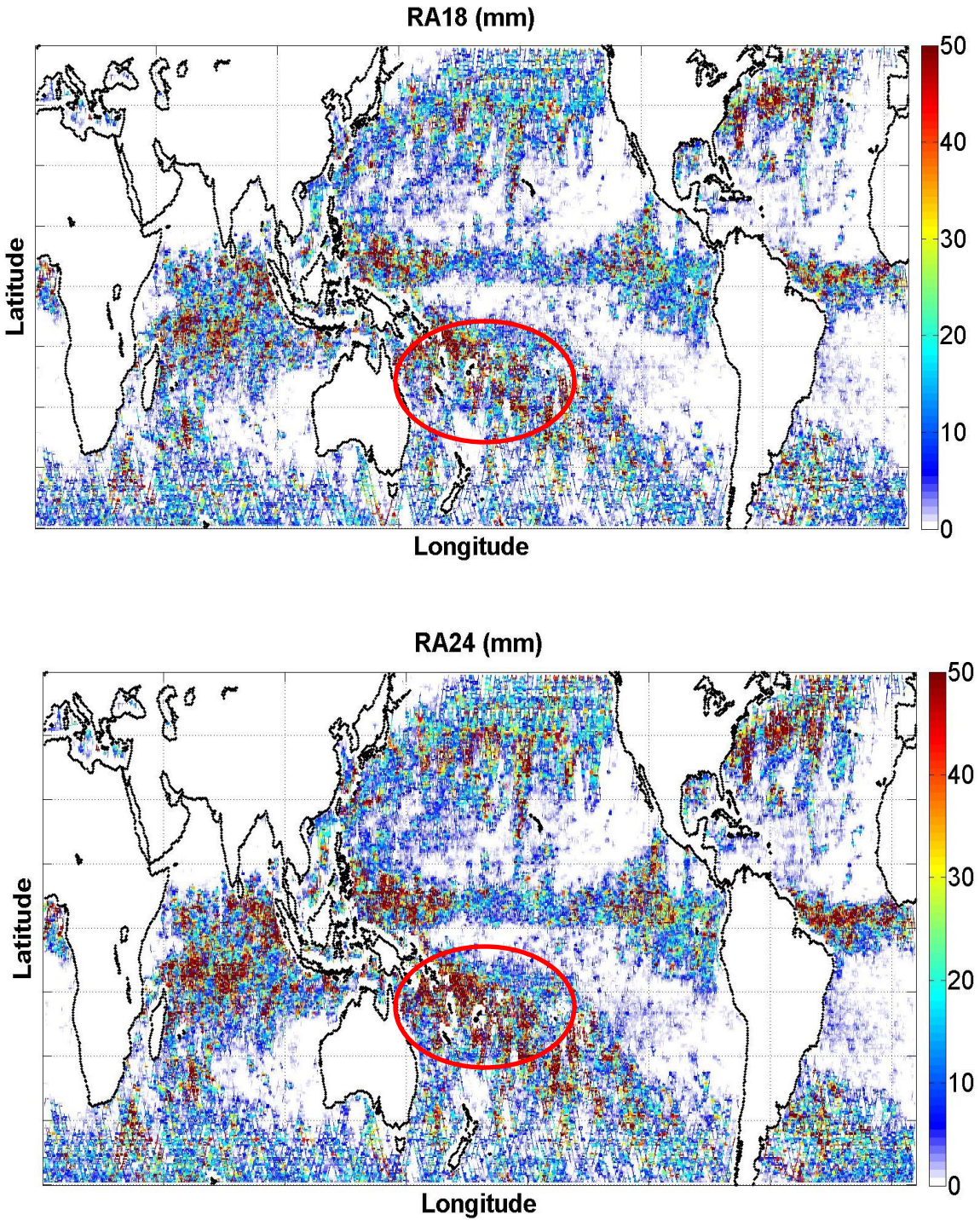

Figure 4.4: Rain accumulation (mm) prior to AQ observation time for 6, 12, 18 and 24 hrs.

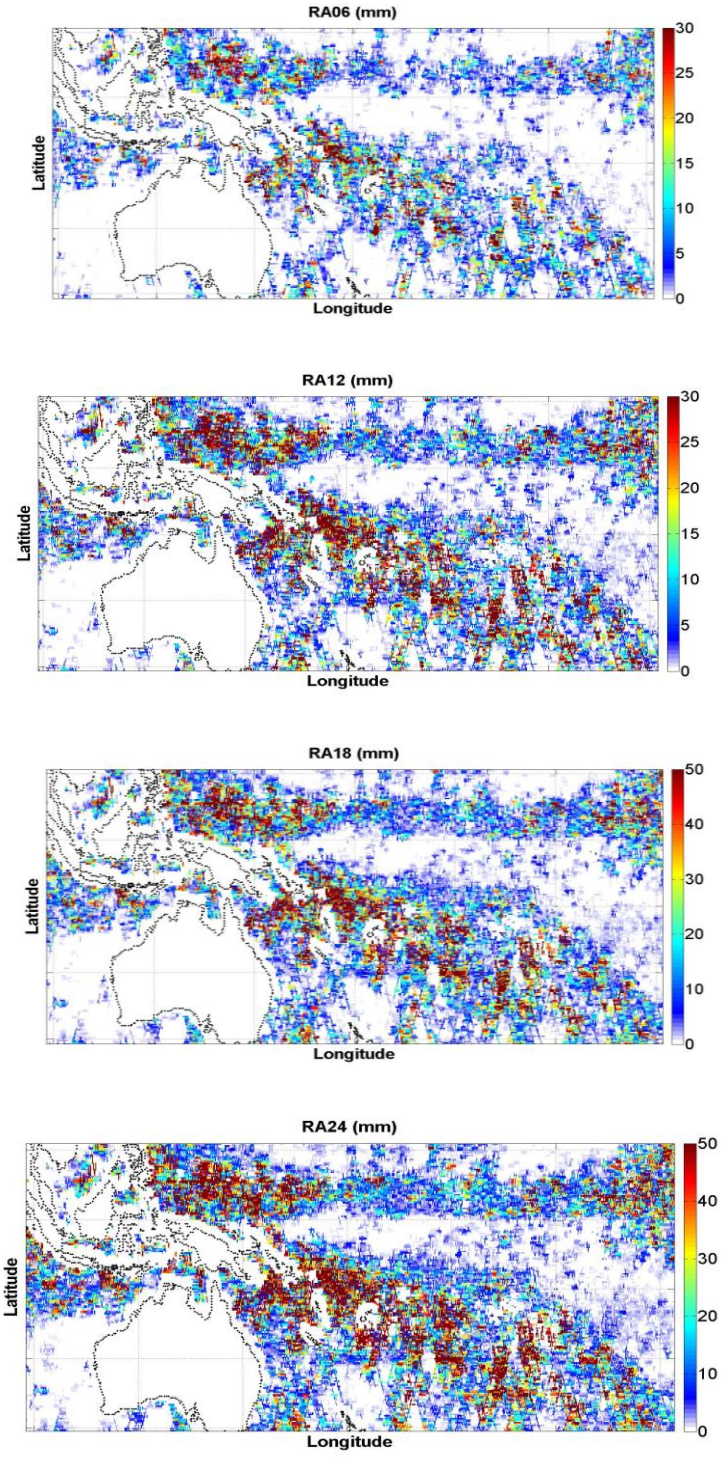

Figure 4.5: Zoomed-in view of rain accumulation (mm) prior to AQ observation time for 6, 12, 18 and 24 hrs.

4.2 Validations

The TRMM 3B42 product has been extensively validated against the TRMM rain retrievals and in situ surface rain gauges [25, 26, 27]. However, it is necessary to validate the interpolated instantaneous rain rate algorithm developed herein. This is performed in a series of "validation experiments" whereby we compare the algorithm outputs against independent rain observations, which are presented in this section.

4.2.1 One 3-hr 3B42 File Interpolation Validation

To validate the 3B42 linear interpolation that we applied in the RA algorithm, we select two 3B42 files from the same day, which are 6 hours apart (for example at 03 and 09hr). Next we apply the linear interpolation to calculate the rain rate at the mid-point (06hr). This interpolated result is expected to be highly correlated to the original 3B42 file at the interpolated time (06hr in this case).

Figure 4.6 shows the rain images for these 2 files where rain rate is shown by color. The top plot is the rain rate image from the original 3B42 file at 06hr and the bottom one is the interpolated rain rate image from 03hr & 09hr at the same time. As expected, from a qualitative visual inspection, they both appear have very similar rain rate patterns.

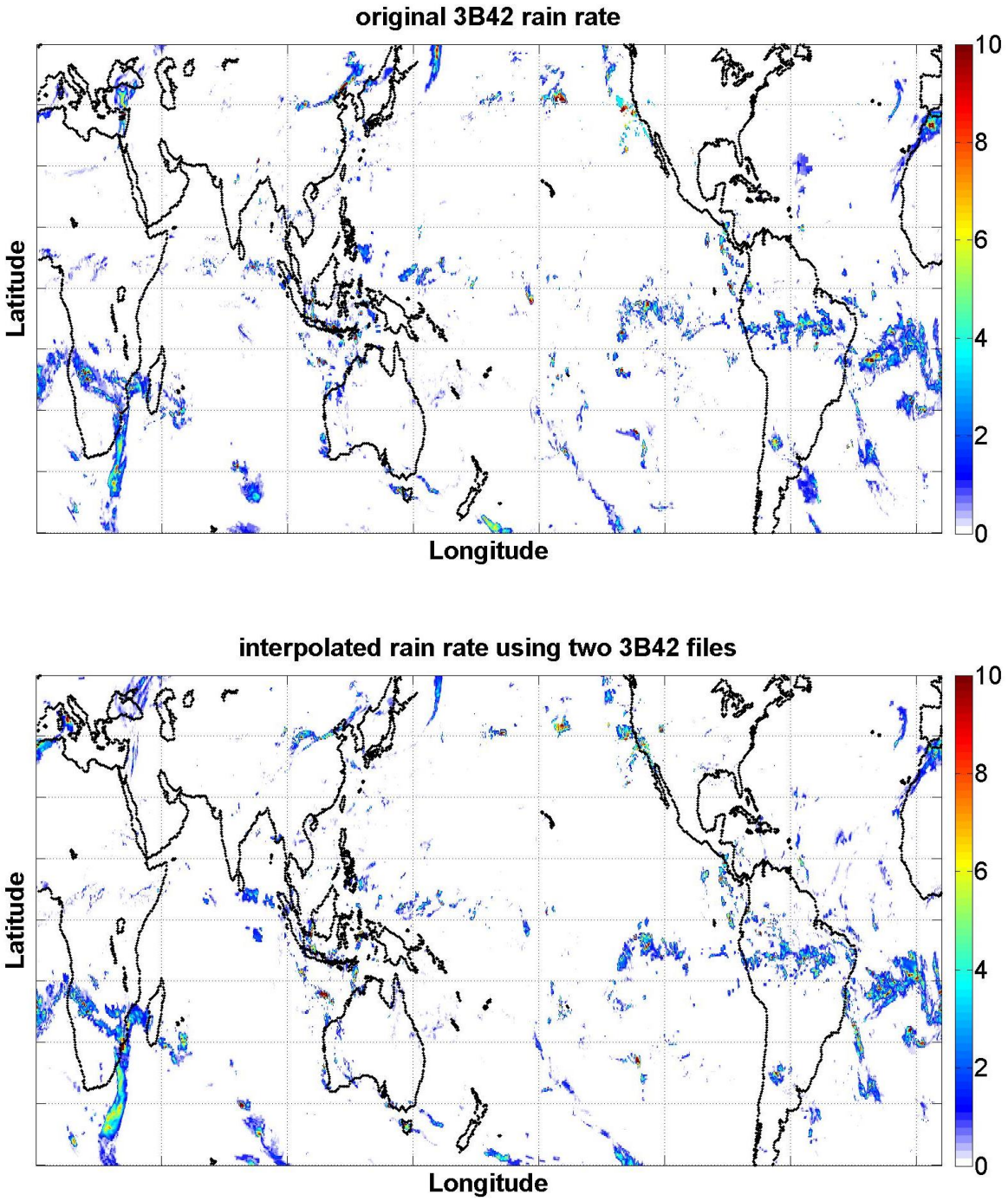

Figure 4.6: The original and interpolated rain rate at 06hr from 3B42 global rain product.

However, to make a more quantitative evaluation, we produce the difference between these two 3B42 rain rate images, and the result is presented in figure 4.7, where the color shows the difference between the original 3B42 rain rate and the interpolated 3B42 rain rate in mm/hr. The differences can be seen better in the expanded image (indicated by the red ellipse) shown in figure 4.8. When examining this differential rain image, there is an apparent spatial displacement in rain patterns exhibited by positive (warm colors) and negative (cool colors) values about the rain event. This means that the assumption of linear changes in time between the intensity of rain events at a 0.25° pixel is not perfect. Rather, it appears that there is a mixture of time variable rain intensity and rain cell displacements caused by the propagating weather patterns.

Figure 4.9 shows the histogram of the difference between the original and interpolated 3B42 rain rate for the same case presented in figure 4.7, where the non-rainy points are excluded.

Figure 4.9: Histogram of the difference between the original and interpolated 3B42 files.

As it is presented in figure 4.9 for the very high percentage of points, (78%) the difference between the original and interpolated 3B42 rain rate lies between ±2mm/hr which indicates a small error for interpolation process.

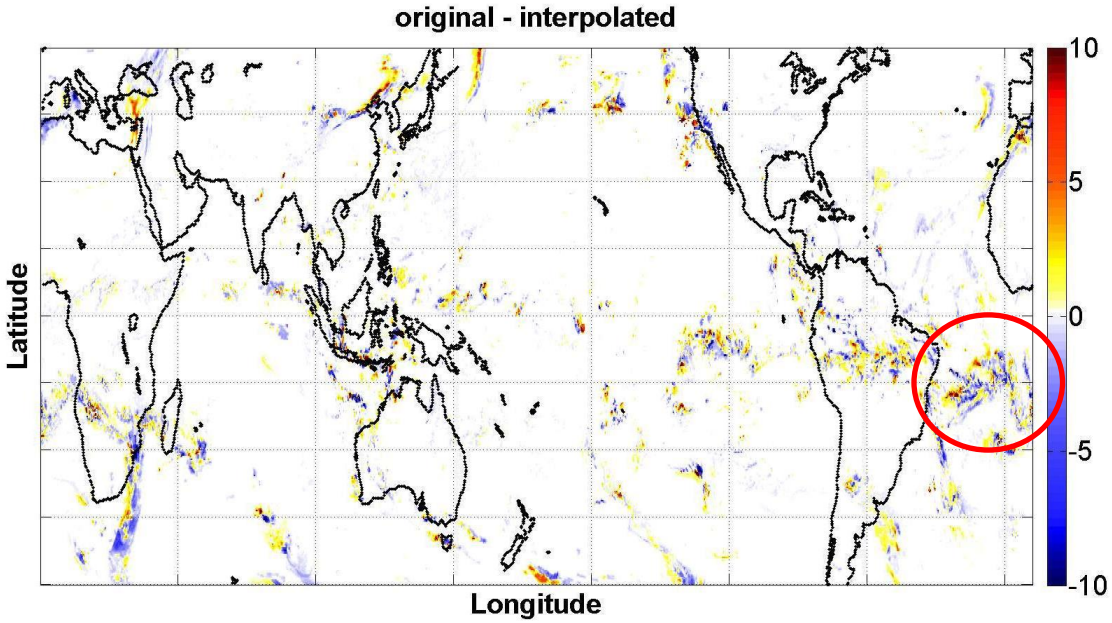

Figure 4.7: Image of the rain rate difference between the original and interpolated 3B42 files at 06hr.

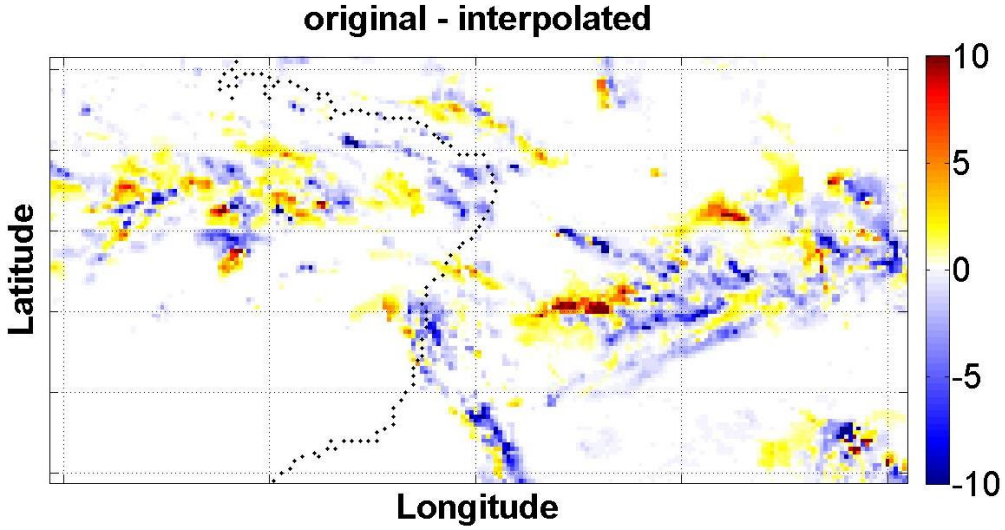

Figure 4.8: Zoomed-in view of the image of the rain rate difference between the original and interpolated 3B42 files at 06hr.

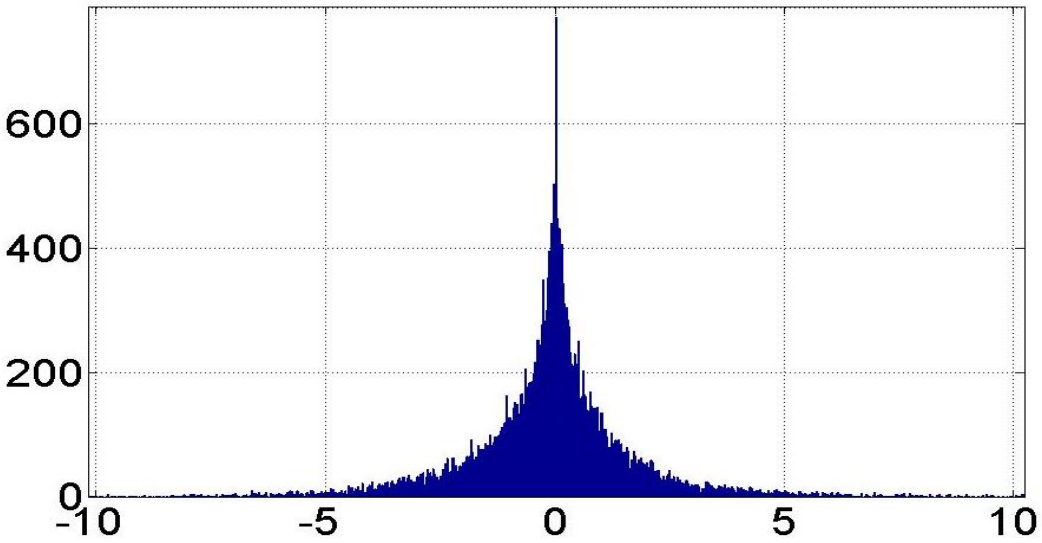

4.2.2 Instantaneous Rain Rate/WindSat EDR Rain Rate Comparisons

To validate the calculation of the instantaneous rain rate (RR), we compare the algorithm output with collocated WindSat Environmental Data Record (EDR) rain rates. To produce the RR, we time interpolate the 3B42 to the closest 15 min window to the AQ observation time and spatially average these values over the AQ IFOV (as described in Section 3.2). For WindSat, we employ a similar procedure whereby the WindSat EDR values are earth gridded and averaged over the AQ IFOV's.

WindSat is a satellite-based polarimetric microwave radiometer developed by the Naval Research Laboratory Remote Sensing Division and the Naval Center for Space Technology [28]. It produces a variety of oceanic and atmospheric environmental parameters including rain rate that are spatially collocated with AQ over a time window of ± 45 min. Further, WindSat rain rates are NOT used to produce 3B42 product; therefore it is a good independent standard for validation.

Orbit by Orbit Basis Comparison of Algorithm RR with WindSat EDR RR

To do an orbit by orbit basis comparison between 3B42 interpolated RR and WindSat EDR RR, the first step is to collocate the earth gridded interpolated 3B42 and WindSat EDR and determine the grids where both 3B42 RR and WindSat EDR RR have observation over AQ footprint on earth. Then the comparison between the linear interpolated 3B42 RR and WindSat EDR is applied by taking the difference between them.

Figure 4.10 shows the global image of the interpolated 3B42 rain rate at AQ observation time over one AQ orbit at the top panel. At the bottom panel a zoomed-in view of the rainy events specified inside the red ellipses are presented for ascending and descending part of the AQ orbit. The color scale shows the interpolated 3B42 rain rate in mm/hr and the swath of AQ footprints is shown in light blue.

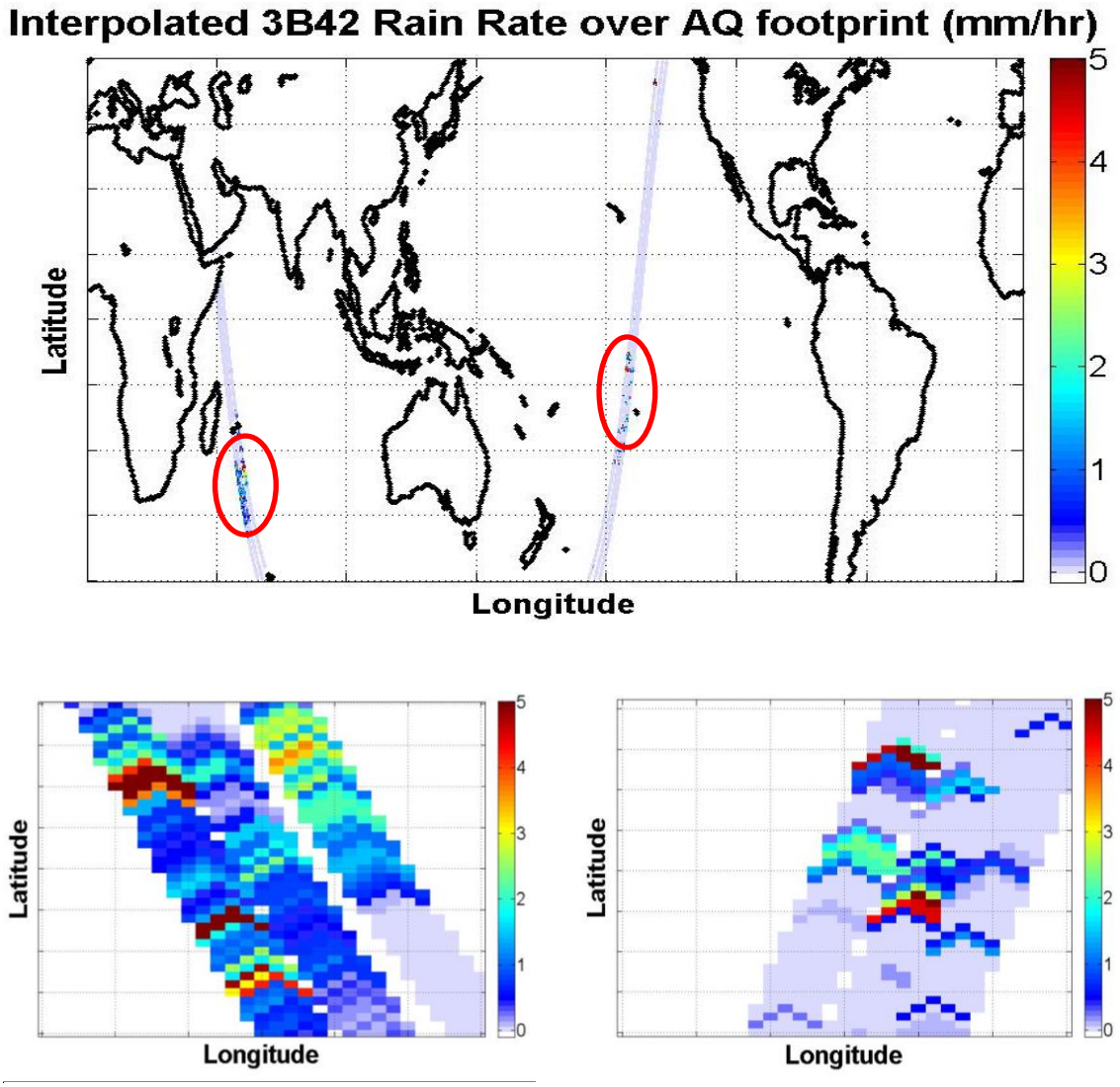

Figure 4.10: Rain image of the interpolated 3B42 rain rate at AQ observation time for one AQ orbit.

Furthermore, in Fig. 4.11 (top panels), the collocated interpolated 3B42 RR (labelled Algorithm RR) over the descending part of the AQ orbit (left panel) and the collocated WindSat EDR RR (right panel) are presented for the same region. It is obvious from

these images that the spatial patterns of rain rate are not the same. Possible reasons will be discussed in Chapter 5.

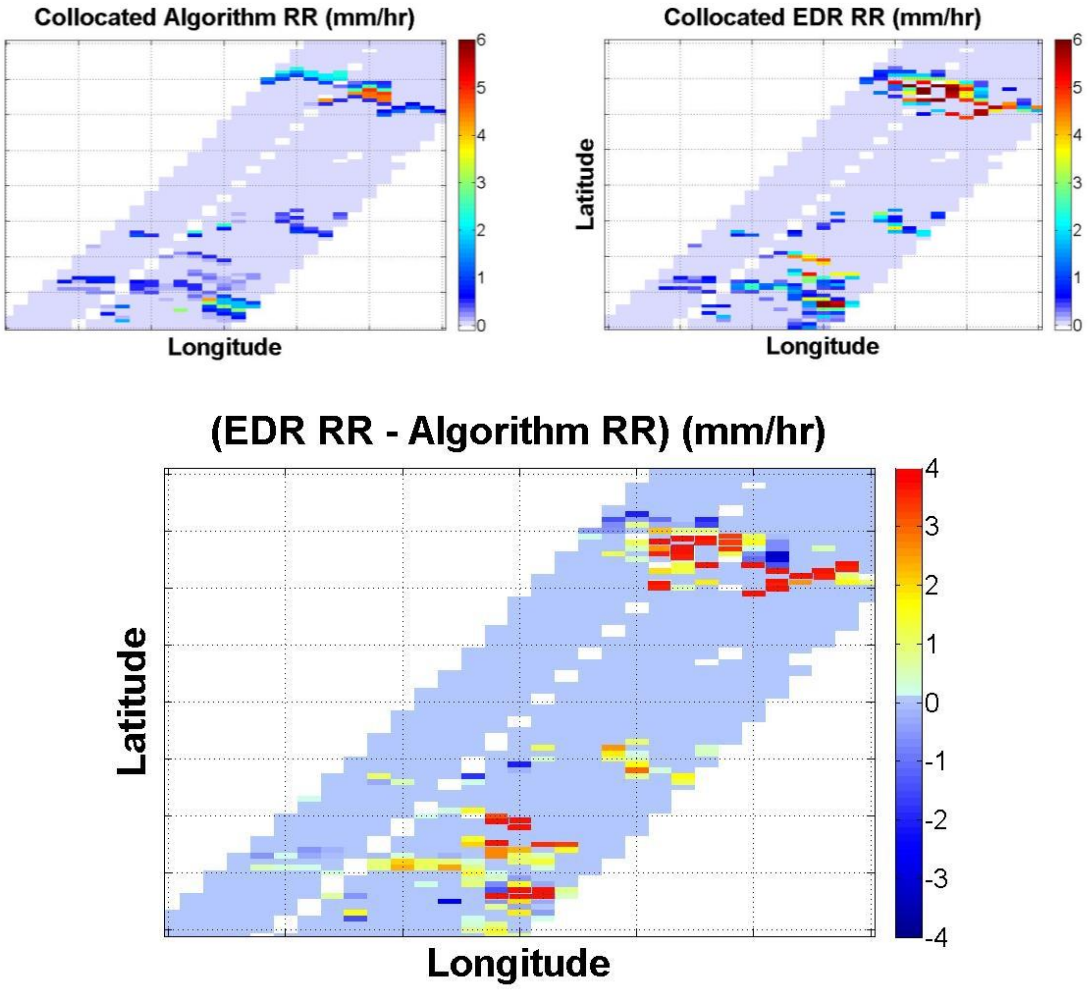

Figure 4.11: Differential rain rate image of (WindSat EDR rain rate) - (Algorithm RR).

In the bottom panel of Fig. 4.11, the difference between RR images is presented. Here the color scale shows the difference between the algorithm RR and WindSat EDR RR in mm/hr. Positive and negative differences are shown by warm and cool colors respectively.

To have a better quantitative understanding of the difference between the interpolated 3B42 RR and WindSat EDR RR; Fig. 4.12 shows the corresponding histogram of Fig. 4.11, where the non-rainy points are excluded.

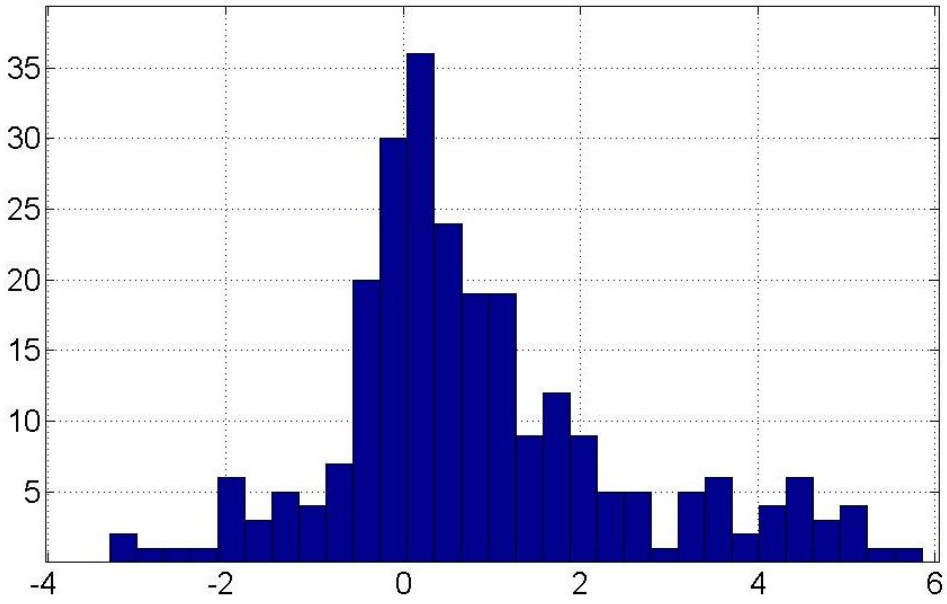

Figure 4.12: Histogram of (the Algorithm rain rate) – (WindSat EDR rain rate), with non-rainy pixels deleted.

Multi-Orbit Basis Comparison of Algorithm RR with WindSat EDR RR

To increase the number of comparisons, results for all the WindSat collocated data in four AQ cycles (~ 7 days in each cycle) are presented in Fig. 4.13. These data are time interpolated 3B42 RR (at the time of the AQ measurements) that have been spatially averaged over the AQ IFOVs and corresponding WindSat EDR RR over the same AQ footprints. Also, the corresponding histogram of Fig. 4.13 is also presented in figure 4.14. For the high percentage of the points (88%) the difference between the collocated points of interpolated 3B42 and WindSat EDR rain rate lies between ±2 mm/hr.

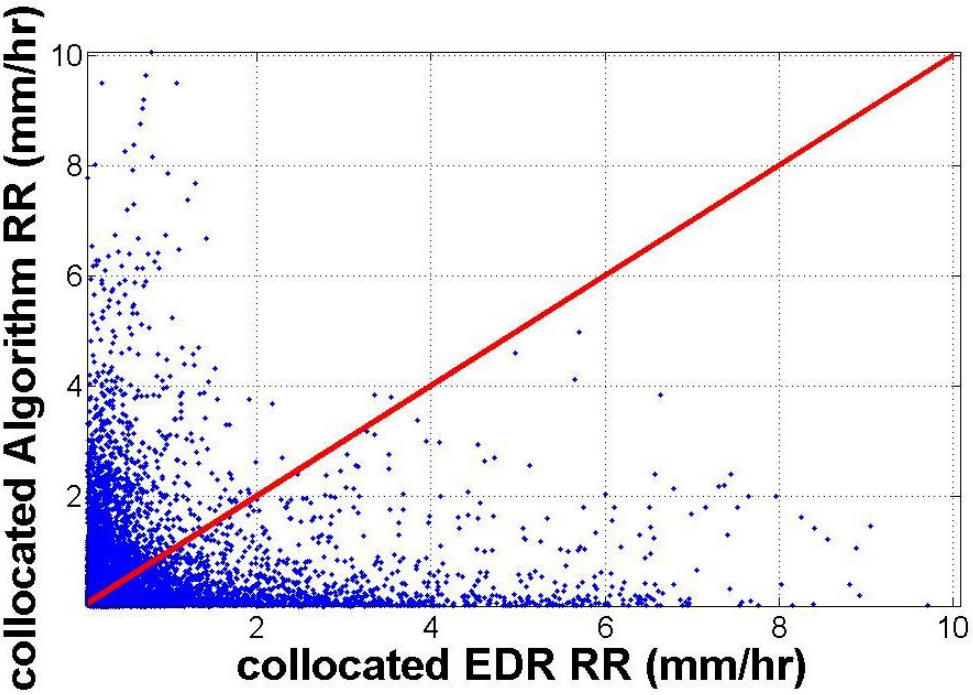

Figure 4.13 Comparison of collocated Algorithm RR with WindSat EDR RR for all orbits in four AQ cycles.

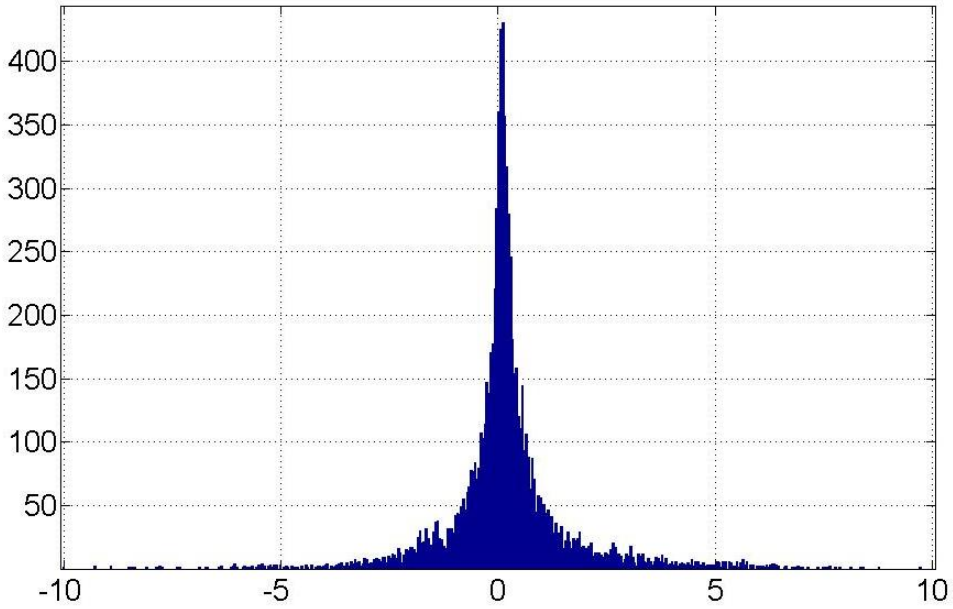

Figure 4.14: Histogram of the difference between the collocated points of Algorithm RR and WindSat EDR RR.

Monthly Average Algorithm Rain Rate with WindSat EDR Rain Rate

In this section, we perform a qualitative evaluation of the monthly averaged algorithm RR using the monthly average of WindSat EDR rain rate as the reference. However, for this comparison, there are significant differences in the spatial resolution and temporal sampling of the WindSat and the RR/RA algorithm. For WindSat, all RR data are averaged over the month (NOT just those collocated with the AQ IFOV's) and the spatial resolution is 0.25° x 0.25°. For the AQ RR/RA algorithm, the cross-track resolution is 1° and the along track spatial sampling is 0.25°. Further, the temporal sampling is global coverage weekly, whereas WindSat achieves global coverage ~ every 2 days. So the spatial patterns of rainfall should only agree well within the large-scale patterns.

Figure 4.15 shows the WindSat EDR monthly averaged rain rate (Feb. 2012) at the top panel and interpolated 3B42 RR average for the same month at the bottom panel. It should be noted that only the area within the yellow box ($\pm 50^{o}$ latitude) should be compared with AQ algorithm RR average.

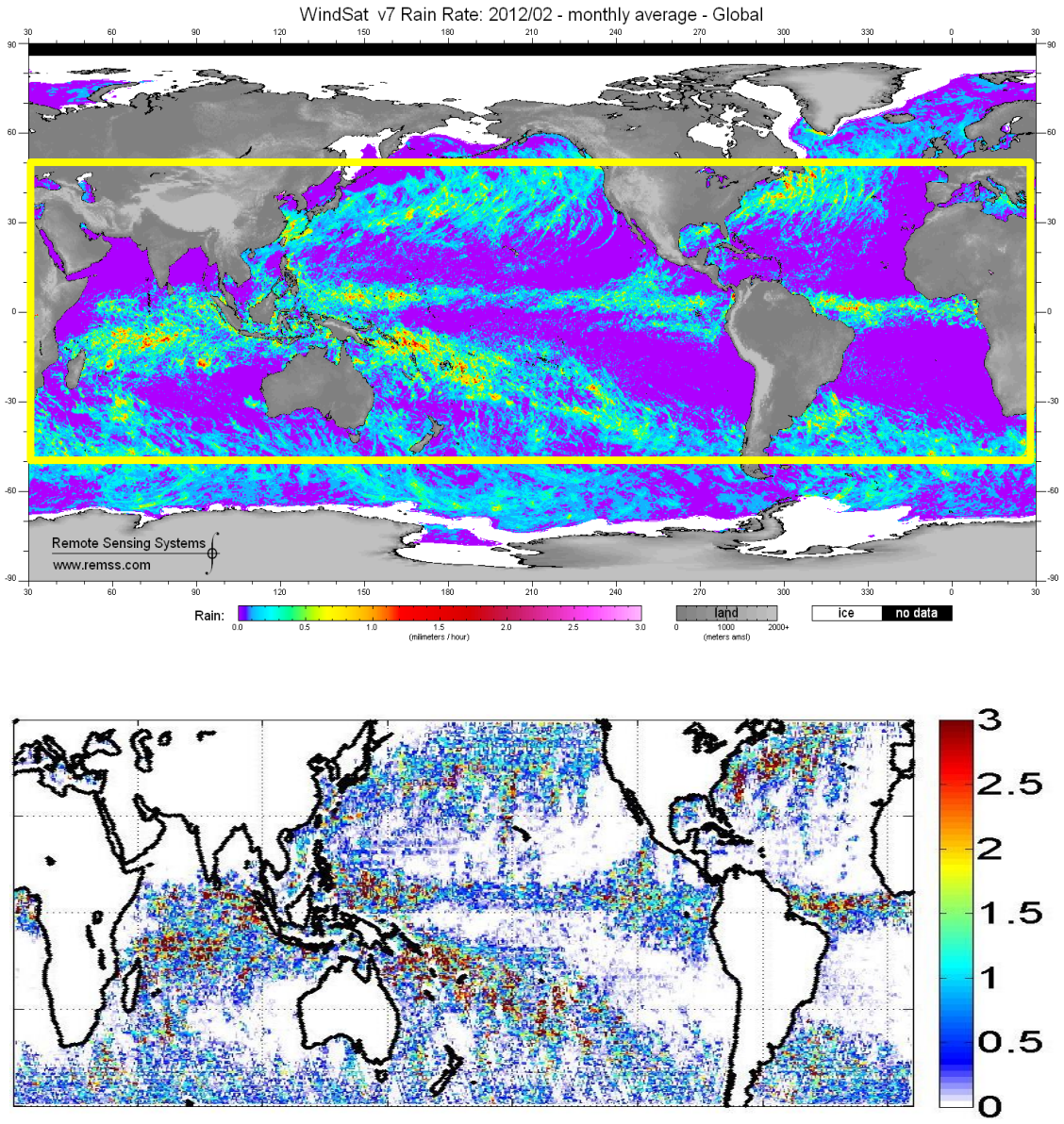

Figure 4.15: Comparison between WindSat EDR monthly averaged rain rate (courtesy of Remote Sensing Systems) and interpolated 3B42 rain rate.

From a qualitative visual inspection, the WindSat image is clearly superior with its higher resolution and greater number of RR samples. Obviously, the AQ monthly averaged RR the image has considerable noise; never-the-less, it captures the monthly rain patterns

quite well. Overall there is very good correlation between these 2 rainfall images, which is encouraging.

CHAPTER 5: CONCLUSIONS AND FUTURE WORK

5.1 Conclusions

An AQ oceanic rainfall accumulation algorithm has been developed to calculate the instantaneous rain rate (RR) and estimate the rain accumulation (RA) in a 3-hr window that has been spatially averaged over the AQ IFOV's. This RR/RA product has the potential to promote better understanding of the effects of rain on the AQ SSS measurements and, as such, can be important to AQ science objectives. We anticipate that this product will provide AQ researchers with scientifically valuable ancillary information about the previous rainfall accumulation that has occurred over an AQ IFOV prior to each Tb measurement. In this regard, this product is unique and, despite the lack of independent validation, is very important.

Based upon preliminary comparison of independent satellite rain measurements from the WindSat radiometer, it is hard to judge the quality of the AQ algorithm RR/RA products. At the rain accumulation (RA) level, there are no independent sources of data that can be used for validation. Further, at the instantaneous RR level, there are other sources, but the lack of higher correlation between 3B42 and WindSat EDR (that have been spatially averaged over AQ IFOV's) is discouraging (e.g., consider Fig. 4.11 and 4.13).

However, this is NOT necessarily a failure of the AQ RR/RA algorithm. This de-correlation may be the result of the heterogeneous nature of rain at theses spatial and temporal scales i.e., 3B42 and WindSat rain rates compared on the 0.25° pixel basis. For

example, in Fig. 4.11 the sampling time for WindSat and the other passive microwave imager used in the 3B42 could easily be ±1 – 2 hours apart. Over this time interval, the rain patterns can move with the prevailing weather patterns over several 0.25° pixel locations. Further because of the dynamic nature of convective rain, the life cycle of a thunderstorm can be of order 30 minutes from genesis to decay. Thus, both of these causes will result in a significant spatial de-correlation of the rain images between WindSat and the 3B42 rain product.

On the other hand, since both 3B42 and WindSat RR compare well in the large-scale and long-time average rainfall patterns (e.g., Fig. 4.15), we are encouraged that the AQ RR/RA product is scientifically meaningful. But the confidence level will remain low until more observations may be compared.

Regardless, it is important to process these data and deliver this unique produce to the AQ scientist and algorithm developers. We have developed an efficient MatLab processing code and prototype RR/RA product generation has begun. These data will be distributed to the AQ Cal/Val team for evaluation starting May 2013.

5.2 Future Work

Most important, the evaluation of the RR/RA produce should continue. More observations are required to develop high confidence estimates of RA errors, under a variety of ocean precipitation conditions. Further, rain characteristics for different rain classifications should be considered. This will require developing an improved global

ocean product than 3B42, which is the plan for the Global Precipitation Mission to be launched next year. There is one such a product known as "CMORPH" (CPC MORPHing) which has better spatial (0.07^{o}) and temporal (30 minutes) resolution compared to the TRMM 3B42, which we will evaluate using [29].

The most important research will be to examine the effect of the RA on the AQ retrieved SSS. For this purpose, a statistical analysis should be performed to develop an empirical relationship between the RA and observed errors in the retrieved SSS. This study would provide experiment evidence that can help AQ algorithm developers to separate the effects of instantaneous and accumulated fresh water on the retrieval of SSS. This would result in an improved SSS retrieval algorithm and reduced measurement error.

Also, there is a possible layered media effect than can affect the smooth ocean Tb. Therefore an electromagnetic model should be developed to calculate the AQ Tb for a lens thickness equal to RA over the oceans. This electromagnetic impedance matching effect can either increase or decrease the smooth ocean emissivity depending upon the thickness of the fresh water layer (RA). Beam fill refraction of rain over AQ IFOV should be also considered.

Since diffusion of salt into fresh water lens caused by rainfall over oceans and mechanical mixing restores the ambient SSS in time, an independent study should be performed to model this procedure. This study will result in to establish an ocean model to estimate the SSS mixing time constant. Wind and waves effects should also be considered the salt mixing time constant.

APPENDIX A: MATLAB SCRIPTS

This appendix contains the MATLAB scripts used to develop RR/RA product.

The first part is the MATLAB code which was used to generate $0.25^{o}\times0.25^{o}$ earth gridded files including the AQ observation time for all AQ three beams. The input to this code is the AQ L-2 file and the output is the earth-gridded AQ observation time for one AQ orbit.

The last part includes the three main codes used to develop RR/RA product over three AQ beams. The earth-gridded AQ observation time and TRMM 3B42 files are the inputs and RR/RA product is the output.

```
%% This code outputs the AQ observation time over AQ footprint in
0.25*0.25 degree resolution %%
%%%%%%%%%% change day number %%%%%%%%%%
%%%%%%%%%% and also change cycle number for different weeks %%%%%%%%%%
%%%%%%%%%% and also change the name of the output file %%%%%%%%%%

clear all; close all;
clc;

disk1 = 'X';
Lon1 = []; Lon2 = []; Lon3 = []; % longitude of the three beams
Lat1 = []; Lat2 = []; Lat3 = []; % latitude of the three beams
AQ_s1 = []; AQ_s2 = []; AQ_s3 = []; % retrieved salinity for 3 beams
ANC_s1 = []; ANC_s2 = []; ANC_s3 = []; % ancillary (HYCOM) salinity for
three beams
t = []; % time of the three beams
count = 0;
dir = [disk1,':\yazan\Aquarius_data\V1.3.1\'];
yrs = ls([dir,'20*']);

for y = 2%:size(yrs,1) % 2 for 2012

    dir_y = [dir,yrs(y,:),'\'];
    dys = ls(dir_y);
    for d = 33 % (Julian day)33 for Feb 2 2012
        dir_d = [dir_y,num2str(d,'%.3d'),'\'];
        files = ls([dir_d,'\Q*1.3.1']);

        for i = 1:size(files,1) % go through all orbits in a day

            name = [dir_d,files(i,:)];

            % Cycle number
            info = hdf5info(name);
            cyc = double(info.GroupHierarchy.Attributes(1,34).Value); %
Cycle Number

            if cyc == 24 % differs for different weeks*****24 for Feb
2-8
                count = count + 1;

                % Navigation
                lon = double(hdf5read(name,'/Navigation/beam_clon')); %
Longitude
                lat = double(hdf5read(name,'/Navigation/beam_clat')); %
Latitude
                sec = double(hdf5read(name,'/Block Attributes/sec')); %
seconds since the beginning of the orbit
                AQ_sss = double(hdf5read(name,'/Aquarius Data/SSS')); %
Aquarius retrieved salinity
                anc_sss=                double(hdf5read(name,'/Aquarius
Data/anc_SSS')); % HYCOM ancillary salinity
```

```
                land          =          double(hdf5read(name,'Aquarius
Data/scat_land_frac')); % scatterometer land fraction
                ice           =          double(hdf5read(name,'Aquarius
Data/scat_ice_frac')); % scatterometer ice fraction

                yr = str2num(files(i,2:5));
                dy = str2num(files(i,6:8));
                time = datenum(yr,0,dy,0,0,sec);

                lon1 = lon(1,:); lon2 = lon(2,:); lon3 = lon(3,:); %
for three beams
                lat1 = lat(1,:); lat2 = lat(2,:); lat3 = lat(3,:);  %
for three beams
                aq_s1 = AQ_sss(1,:); aq_s2 = AQ_sss(2,:); aq_s3 =
AQ_sss(3,:); % for three beams
                anc_s1 = anc_sss(1,:); anc_s2 = anc_sss(2,:); anc_s3 =
anc_sss(3,:); % for three beams
                lnd1 = land(1,:); lnd2 = land(2,:); lnd3 = land(3,:);
                ice1 = ice(1,:); ice2 = ice(2,:); ice3 = ice(3,:);

                %% Filter the data
                n1 = find(aq_s1>0 & lnd1>=0 & lnd1<=1e-3 & ice1>=0 &
ice1<=1e-3);
                n2 = find(aq_s2>0 & lnd2>=0 & lnd2<=1e-3 & ice2>=0 &
ice2<=1e-3);
                n3 = find(aq_s3>0 & lnd3>=0 & lnd3<=1e-3 & ice3>=0 &
ice3<=1e-3);

                %% combine data
                Lon1 = [Lon1 , lon1(n1)]; Lon2 = [Lon2 , lon2(n2)];
Lon3 = [Lon3 , lon3(n3)];
                Lat1 = [Lat1 , lat1(n1)]; Lat2 = [Lat2 , lat2(n2)];
Lat3 = [Lat3 , lat3(n3)];
                t = [t , time'];
                AQ_s1 = [AQ_s1 , aq_s1(n1)];    AQ_s2 = [AQ_s2 ,
aq_s2(n2)]; AQ_s3 = [AQ_s3 , aq_s3(n3)];
                ANC_s1 = [ANC_s1 , anc_s1(n1)]; ANC_s2 = [ANC_s2 ,
anc_s2(n2)]; ANC_s3 = [ANC_s3 , anc_s3(n3)];

                if count==103
                    break;
                end
            end
            eg1     =     earth_grid_180(Lat1,Lon1,t,0.25);     eg1     =
eg1(161:560,:); % do gridding for time for beam1
            eg2     =     earth_grid_180(Lat2,Lon2,t,0.25);     eg2     =
eg2(161:560,:); % do gridding for time for beam2
            eg3     =     earth_grid_180(Lat3,Lon3,t,0.25);     eg3     =
eg3(161:560,:); % do gridding for time for beam3

            save(['J:\foldar_name\grid_20120202_'   ,num2str(i,'%0.2d')]
, 'eg1','eg2','eg3');
```

```
            clearvars -except disk1 count dir yrs y dir_y dys a b d
dir_d files
            Lon1 = []; Lon2 = []; Lon3 = []; % longitude of the three
beams
            Lat1 = []; Lat2 = []; Lat3 = []; % latitude of the three
beams
            AQ_s1 = []; AQ_s2 = []; AQ_s3 = []; % retrieved salinity
for 3 beams
            ANC_s1 = []; ANC_s2 = []; ANC_s3 = []; % ancillary salinity
for three beams
            t = []; % time of the three beams
        end
    end
end


function [eg_data] = earth_grid_180(lat,lon,data,res)
%lat: latitude vector
%lon: longitude vector
%data: data to be gridded vector
%res: resolution of earth gridding

% tic
lat=lat(:); lon=lon(:); data= data(:);
sz = size(lat,1);

% reconvert the lon( 0 -> 360) and lat (0->181)
lon(lon<0) = 360+(lon(lon<0));
lon_ind = lon+1;
lon_ind(lon_ind>360) = 360;

lat = 90+lat;
lat_ind = lat+1;

a = floor(180/res);
b = floor(360/res);
% create an empty sheets to earth grid on them
count = zeros(a,b);
eg_data = zeros(a,b);

for i=1:sz
    m1 = floor(lat_ind(i)/res);
    m = a-m1;
    n = floor(lon_ind(i)/res);

    eg_data(m,n) = eg_data(m,n) + data(i);
    count(m,n) = count(m,n)+1;
end

eg_data(count>0) = eg_data(count>0)./count(count>0);
% toc
return
```

```
%%%%%%%%%% this code calculates the earth gridded RR, RA03, RA06, RA09,
RA12, RA15, RA18, RA21, and RA24 for AQ beam#1 %%%%%%%%%%
%%%%%%%%%% Do not forget to change the day and month number %%%%%%%%%%
close all;
clear all;clc;
tic
for rev = 1:15
day = 2;
load(['J:\folder_name\AQ_grid\grid_201202'    ,num2str(day,'%0.2d'),'_',
num2str(rev,'%0.2d') , '.mat']); % AQ time grid

res = 0.25;
a = [1:7/96:8]; % create the required points for time interpolation
every 15 minutes for 24-hr time period

%%%%% load 3B42 rain rates every 3-hr for 24 hour for previous day
P1 = [];
for k = 1:8
    filename=(['J:\folder_name\data_mirador\3B42.201202'   ,num2str(day-
1,'%0.2d') , '.' ,num2str(3*k-3,'%0.2d'), '.7.HDF']);
    P_K   =   rot90(   double(hdfread(filename',   '/Grid/precipitation',
'Index', {[1  1],[1  1],[1440   400]})) ) ; P_K(P_K(:,:)<0)=NaN;
    per = P_K;
    per1 = per(:,1:(180/res));
    per2 = per(:,((180/res)+1):end);
    P_K = [per2 , per1];
    P1 = cat(3,P1,P_K);
end
%%%%%%%%%% to interpolate 3B42 RR every 15 min %%%%%%%%%%
P1_new = zeros(400,1440,size(a,2));
for row = 1:400
    for col = 1:1440
        x1 = P1(row,col,:);
        x1 = reshape(x1,1,8);
        y1 = interp1(x1,a);
        P1_new (row,col,:) = reshape(y1,1,1,size(a,2));
    end
end
%%%%% load 3B42 rain rates every 3-hr for 24 hour for current day
P2 = [];
for k = 1:8
    filename=(['J:\folder_name\data_mirador\3B42.201202'
,num2str(day,'%0.2d'), '.' ,num2str(3*k-3,'%0.2d'), '.7.HDF']);
    P_K   =   rot90(   double(hdfread(filename',   '/Grid/precipitation',
'Index', {[1  1],[1  1],[1440   400]})) ) ; P_K(P_K(:,:)<0)=NaN;
    per = P_K;
    per1 = per(:,1:(180/res));
    per2 = per(:,((180/res)+1):end);
    P_K = [per2 , per1];
    P2 = cat(3,P2,P_K);
end
%%%%%%%%%% to interpolate 3B42 RR every 15 min %%%%%%%%%%
P2_new = zeros(400,1440,size(a,2));
```

```
for row = 1:400
    for col = 1:1440
        x2 = P2(row,col,:);
        x2 = reshape(x2,1,8);
        y2 = interp1(x2,a);
        P2_new (row,col,:) = reshape(y2,1,1,size(a,2));
    end
end

precipitation_new = cat(3,P1_new,P2_new); % interpolated 3B42 RR (every
15 min) for previous and current day

sample_time = [0:0.25:24]; % 0-24 hr every 15 min

RR = zeros(400,1440);
%%%%% create empty sheets for grd_RR_ii every 15 min %%%%%
for i =1:97
    eval(['RR' num2str(i,'%0.2d') '=zeros(400,1440);']);
end

for a = 3:398
    for b = 3:1438
        if eg1(a,b)~=0
            aq_time = datevec(eg1(a,b));
            aq_t = aq_time(4) + (aq_time(5)/60);
            pick = abs(sample_time - aq_t);
            id  =  min(find(pick==(min(pick))));  %  min  added  for  the
cases which we have to id's
            for i=1:97
                eval(['RR'num2str(i,'%0.2d')'(a,b)=
(precipitation_new(a-2,b,id+97-i)+precipitation_new(a-1,b-1,id+97-
i)+precipitation_new(a-1,b,id+97-i)+precipitation_new(a-1,b+1,id+97-
i)+'precipitation_new(a,b-2,id+97-i)+precipitation_new(a,b-1,id+97-
i)+precipitation_new(a,b,id+97-i)+precipitation_new(a,b+1,id+97-
i)+precipitation_new(a,b+2,id+97-i)+precipitation_new(a+1,b-1,id+97-
i)+'precipitation_new(a+1,b,id+97-i)+precipitation_new(a+1,b+1,id+97-
i)+precipitation_new(a+2,b,id+97-i))/13;']);
            end
            RR(a,b)=(precipitation_new(a-
2,b,id+97)+precipitation_new(a-1,b-1,id+97)+precipitation_new(a-
1,b,id+97)+precipitation_new(a-1,b+1,id+97)+precipitation_new(a,b-
2,id+97)+precipitation_new(a,b-1,id+97)+
precipitation_new(a,b,id+97)+precipitation_new(a,b+1,id+97)+precipitati
on_new(a,b+2,id+97)+precipitation_new(a+1,b-1,id+97)
+precipitation_new(a+1,b,id+97)+precipitation_new(a+1,b+1,id+97)+precip
itation_new(a+2,b,id+97))/13;
        end
    end
end

%%%%%%%% Create empty sheets to calculate Rain Accumulation %%%%%%%%%%
RA03 = zeros(400,1440); RA06 = zeros(400,1440); RA09 = zeros(400,1440);
RA12 = zeros(400,1440);
```

```
RA15 = zeros(400,1440); RA18 = zeros(400,1440); RA21 = zeros(400,1440);
RA24 = zeros(400,1440);
%%%%%%%% calculate Rain Accumulation %%%%%%%%%%
for i = 2:13
    eval(['RA03 = RA03 + RR' num2str(i,'%0.2d') '*0.25;']);
end

for i = 2:25
    eval(['RA06 = RA06 + RR' num2str(i,'%0.2d') '*0.25;']);
end

for i = 2:37
    eval(['RA09 = RA09 + RR' num2str(i,'%0.2d') '*0.25;']);
end

for i = 2:49
    eval(['RA12 = RA12 + RR' num2str(i,'%0.2d') '*0.25;']);
end

for i = 2:61
    eval(['RA15 = RA15 + RR' num2str(i,'%0.2d') '*0.25;']);
end

for i = 2:73
    eval(['RA18 = RA18 + RR' num2str(i,'%0.2d') '*0.25;']);
end

for i = 2:85
    eval(['RA21 = RA21 + RR' num2str(i,'%0.2d') '*0.25;']);
end

for i = 2:97
    eval(['RA24 = RA24 + RR' num2str(i,'%0.2d') '*0.25;']);
end

save(['J:\folder_name\AQ_IRR_delSSS\IRR_delSSS_201205'
,num2str(day,'%0.2d'),'_', num2str(rev,'%0.2d'), '_B1'] ,...
    'RR','RA03','RA06','RA09','RA12','RA15','RA18','RA21','RA24');
clear all;
end
```

```
%%%%%%%%%% this code calculates the earth gridded RR, RA03, RA06, RA09,
RA12, RA15, RA18, RA21, and RA24 for AQ beam#2 %%%%%%%%%%
%%%%%%%%%% Do not forget to change the day and month number %%%%%%%%%%
close all;
clear all;clc;
tic
for rev = 1:15
day = 2;
load(['J:\folder_name\AQ_grid\grid_201202'    ,num2str(day,'%0.2d'),'_',
num2str(rev,'%0.2d') , '.mat']); % AQ time grid

res = 0.25;
a = [1:7/96:8]; % create the required points for time interpolation
every 15 minutes for 24-hr time period

%%%%% load 3B42 rain rates every 3-hr for 24 hour for previous day
P1 = [];
for k = 1:8
    filename=(['J:\folder_name\data_mirador\3B42.201202'   ,num2str(day-
1,'%0.2d') , '.' ,num2str(3*k-3,'%0.2d'), '.7.HDF']);
    P_K   =   rot90(   double(hdfread(filename',   '/Grid/precipitation',
'Index', {[1  1],[1  1],[1440   400]})) ) ; P_K(P_K(:,:)<0)=NaN;
    per = P_K;
    per1 = per(:,1:(180/res));
    per2 = per(:,((180/res)+1):end);
    P_K = [per2 , per1];
    P1 = cat(3,P1,P_K);
end
%%%%%%%%%% to interpolate 3B42 RR every 15 min %%%%%%%%%%
P1_new = zeros(400,1440,size(a,2));
for row = 1:400
    for col = 1:1440
        x1 = P1(row,col,:);
        x1 = reshape(x1,1,8);
        y1 = interp1(x1,a);
        P1_new (row,col,:) = reshape(y1,1,1,size(a,2));
    end
end
%%%%% load 3B42 rain rates every 3-hr for 24 hour for current day
P2 = [];
for k = 1:8
    filename=(['J:\folder_name\data_mirador\3B42.201202'
,num2str(day,'%0.2d'), '.' ,num2str(3*k-3,'%0.2d'), '.7.HDF']);
    P_K   =   rot90(   double(hdfread(filename',   '/Grid/precipitation',
'Index', {[1  1],[1  1],[1440   400]})) ) ; P_K(P_K(:,:)<0)=NaN;
    per = P_K;
    per1 = per(:,1:(180/res));
    per2 = per(:,((180/res)+1):end);
    P_K = [per2 , per1];
    P2 = cat(3,P2,P_K);
end
%%%%%%%%%% to interpolate 3B42 RR every 15 min %%%%%%%%%%
P2_new = zeros(400,1440,size(a,2));
```

```
for row = 1:400
    for col = 1:1440
        x2 = P2(row,col,:);
        x2 = reshape(x2,1,8);
        y2 = interp1(x2,a);
        P2_new (row,col,:) = reshape(y2,1,1,size(a,2));
    end
end

precipitation_new = cat(3,P1_new,P2_new); % interpolated 3B42 RR (every
15 min) for previous and current day

sample_time = [0:0.25:24]; % 0-24 hr every 15 min

RR = zeros(400,1440);
%%%%% create empty sheets for grd_RR_ii every 15 min %%%%%
for i =1:97
    eval(['RR' num2str(i,'%0.2d') '=zeros(400,1440);']);
end

for a = 3:398
    for b = 3:1438
        if eg2(a,b)~=0
            aq_time = datevec(eg2(a,b));
            aq_t = aq_time(4) + (aq_time(5)/60);
            pick = abs(sample_time - aq_t);
            id  =  min(find(pick==(min(pick))));  %  min  added  for  the
cases which we have to id's
            for i=1:97
                eval(['RR'num2str(i,'%0.2d')'(a,b)=
(precipitation_new(a-2,b,id+97-i)+precipitation_new(a-1,b-1,id+97-
i)+precipitation_new(a-1,b,id+97-i)+precipitation_new(a-1,b+1,id+97-
i)+'precipitation_new(a,b-2,id+97-i)+precipitation_new(a,b-1,id+97-
i)+precipitation_new(a,b,id+97-i)+precipitation_new(a,b+1,id+97-
i)+precipitation_new(a,b+2,id+97-i)+precipitation_new(a+1,b-1,id+97-
i)+'precipitation_new(a+1,b,id+97-i)+precipitation_new(a+1,b+1,id+97-
i)+precipitation_new(a+2,b,id+97-i))/13;']);
            end
            RR(a,b)=(precipitation_new(a-
2,b,id+97)+precipitation_new(a-1,b-1,id+97)+precipitation_new(a-
1,b,id+97)+precipitation_new(a-1,b+1,id+97)+precipitation_new(a,b-
2,id+97)+precipitation_new(a,b-1,id+97)+
precipitation_new(a,b,id+97)+precipitation_new(a,b+1,id+97)+precipitati
on_new(a,b+2,id+97)+precipitation_new(a+1,b-1,id+97)
+precipitation_new(a+1,b,id+97)+precipitation_new(a+1,b+1,id+97)+precip
itation_new(a+2,b,id+97))/13;
        end
    end
end

%%%%%%%% create empty sheets to calculate Rain Accumulation %%%%%%%%%%
RA03 = zeros(400,1440); RA06 = zeros(400,1440); RA09 = zeros(400,1440);
RA12 = zeros(400,1440);
```

```
RA15 = zeros(400,1440); RA18 = zeros(400,1440); RA21 = zeros(400,1440);
RA24 = zeros(400,1440);
%%%%%%%% calculate Rain Accumulation %%%%%%%%%%
for i = 2:13
    eval(['RA03 = RA03 + RR' num2str(i,'%0.2d') '*0.25;']);
end

for i = 2:25
    eval(['RA06 = RA06 + RR' num2str(i,'%0.2d') '*0.25;']);
end

for i = 2:37
    eval(['RA09 = RA09 + RR' num2str(i,'%0.2d') '*0.25;']);
end

for i = 2:49
    eval(['RA12 = RA12 + RR' num2str(i,'%0.2d') '*0.25;']);
end

for i = 2:61
    eval(['RA15 = RA15 + RR' num2str(i,'%0.2d') '*0.25;']);
end

for i = 2:73
    eval(['RA18 = RA18 + RR' num2str(i,'%0.2d') '*0.25;']);
end

for i = 2:85
    eval(['RA21 = RA21 + RR' num2str(i,'%0.2d') '*0.25;']);
end

for i = 2:97
    eval(['RA24 = RA24 + RR' num2str(i,'%0.2d') '*0.25;']);
end

save(['J:\folder_name\AQ_IRR_delSSS\IRR_delSSS_201205'
,num2str(day,'%0.2d'),'_', num2str(rev,'%0.2d'), '_B1'] ,...
    'RR','RA03','RA06','RA09','RA12','RA15','RA18','RA21','RA24');
clear all;
end
toc
```

```
%%%%%%%%%% this code calculates the earth gridded RR, RA03, RA06, RA09,
RA12, RA15, RA18, RA21, and RA24 for AQ beam#3 %%%%%%%%%%
%%%%%%%%%% Do not forget to change the day and month number %%%%%%%%%%
close all;
clear all;clc;
tic
for rev = 1:15
day = 2;
load(['J:\folder_name\AQ_grid\grid_201202'    ,num2str(day,'%0.2d'),'_',
num2str(rev,'%0.2d') , '.mat']); % AQ time grid

res = 0.25;
a = [1:7/96:8]; % create the required points for time interpolation
every 15 minutes for 24-hr time period

%%%%% load 3B42 rain rates every 3-hr for 24 hour for previous day
P1 = [];
for k = 1:8
    filename=(['J:\folder_name\data_mirador\3B42.201202'   ,num2str(day-
1,'%0.2d') , '.' ,num2str(3*k-3,'%0.2d'), '.7.HDF']);
    P_K   =   rot90(   double(hdfread(filename',   '/Grid/precipitation',
'Index', {[1  1],[1  1],[1440   400]})) ) ; P_K(P_K(:,:)<0)=NaN;
    per = P_K;
    per1 = per(:,1:(180/res));
    per2 = per(:,((180/res)+1):end);
    P_K = [per2 , per1];
    P1 = cat(3,P1,P_K);
end
%%%%%%%%%% to interpolate 3B42 RR every 15 min %%%%%%%%%%
P1_new = zeros(400,1440,size(a,2));
for row = 1:400
    for col = 1:1440
        x1 = P1(row,col,:);
        x1 = reshape(x1,1,8);
        y1 = interp1(x1,a);
        P1_new (row,col,:) = reshape(y1,1,1,size(a,2));
    end
end
%%%%% load 3B42 rain rates every 3-hr for 24 hour for current day
P2 = [];
for k = 1:8
    filename=(['J:\folder_name\data_mirador\3B42.201202'
,num2str(day,'%0.2d'), '.' ,num2str(3*k-3,'%0.2d'), '.7.HDF']);
    P_K   =   rot90(   double(hdfread(filename',   '/Grid/precipitation',
'Index', {[1  1],[1  1],[1440   400]})) ) ; P_K(P_K(:,:)<0)=NaN;
    per = P_K;
    per1 = per(:,1:(180/res));
    per2 = per(:,((180/res)+1):end);
    P_K = [per2 , per1];
    P2 = cat(3,P2,P_K);
end
%%%%%%%%%% to interpolate 3B42 RR every 15 min %%%%%%%%%%
P2_new = zeros(400,1440,size(a,2));
```

```
for row = 1:400
    for col = 1:1440
        x2 = P2(row,col,:);
        x2 = reshape(x2,1,8);
        y2 = interp1(x2,a);
        P2_new (row,col,:) = reshape(y2,1,1,size(a,2));
    end
end

precipitation_new = cat(3,P1_new,P2_new); % interpolated 3B42 RR (every
15 min) for previous and current day

sample_time = [0:0.25:24]; % 0-24 hr every 15 min

RR = zeros(400,1440);
%%%%% create empty sheets for grd_RR_ii every 15 min %%%%%
for i =1:97
    eval(['RR' num2str(i,'%0.2d') '=zeros(400,1440);']);
end

for a = 3:398
    for b = 3:1438
        if eg3(a,b)~=0
            aq_time = datevec(eg3(a,b));
            aq_t = aq_time(4) + (aq_time(5)/60);
            pick = abs(sample_time - aq_t);
            id  =  min(find(pick==(min(pick))));  %  min  added  for  the
cases which we have to id's
            for i=1:97
                eval(['RR'num2str(i,'%0.2d')'(a,b)=
(precipitation_new(a-2,b,id+97-i)+precipitation_new(a-1,b-1,id+97-
i)+precipitation_new(a-1,b,id+97-i)+precipitation_new(a-1,b+1,id+97-
i)+'precipitation_new(a,b-2,id+97-i)+precipitation_new(a,b-1,id+97-
i)+precipitation_new(a,b,id+97-i)+precipitation_new(a,b+1,id+97-
i)+precipitation_new(a,b+2,id+97-i)+precipitation_new(a+1,b-1,id+97-
i)+'precipitation_new(a+1,b,id+97-i)+precipitation_new(a+1,b+1,id+97-
i)+precipitation_new(a+2,b,id+97-i))/13;']);
            end
            RR(a,b)=(precipitation_new(a-
2,b,id+97)+precipitation_new(a-1,b-1,id+97)+precipitation_new(a-
1,b,id+97)+precipitation_new(a-1,b+1,id+97)+precipitation_new(a,b-
2,id+97)+precipitation_new(a,b-1,id+97)+
precipitation_new(a,b,id+97)+precipitation_new(a,b+1,id+97)+precipitati
on_new(a,b+2,id+97)+precipitation_new(a+1,b-1,id+97)
+precipitation_new(a+1,b,id+97)+precipitation_new(a+1,b+1,id+97)+precip
itation_new(a+2,b,id+97))/13;
        end
    end
end

%%%%%%%% create empty sheets to calculate Rain Accumulation %%%%%%%%%%
RA03 = zeros(400,1440); RA06 = zeros(400,1440); RA09 = zeros(400,1440);
RA12 = zeros(400,1440);
```

```
RA15 = zeros(400,1440); RA18 = zeros(400,1440); RA21 = zeros(400,1440);
RA24 = zeros(400,1440);
%%%%%%%% calculate Rain Accumulation %%%%%%%%%%
for i = 2:13
    eval(['RA03 = RA03 + RR' num2str(i,'%0.2d') '*0.25;']);
end

for i = 2:25
    eval(['RA06 = RA06 + RR' num2str(i,'%0.2d') '*0.25;']);
end

for i = 2:37
    eval(['RA09 = RA09 + RR' num2str(i,'%0.2d') '*0.25;']);
end

for i = 2:49
    eval(['RA12 = RA12 + RR' num2str(i,'%0.2d') '*0.25;']);
end

for i = 2:61
    eval(['RA15 = RA15 + RR' num2str(i,'%0.2d') '*0.25;']);
end

for i = 2:73
    eval(['RA18 = RA18 + RR' num2str(i,'%0.2d') '*0.25;']);
end

for i = 2:85
    eval(['RA21 = RA21 + RR' num2str(i,'%0.2d') '*0.25;']);
end

for i = 2:97
    eval(['RA24 = RA24 + RR' num2str(i,'%0.2d') '*0.25;']);
end

save(['J:\folder_name\AQ_IRR_delSSS\IRR_delSSS_201205'
,num2str(day,'%0.2d'),'_', num2str(rev,'%0.2d'), '_B1'] ,...
    'RR','RA03','RA06','RA09','RA12','RA15','RA18','RA21','RA24');
clear all;
end
toc
```

REFERENCES

[1] Le Vine, D.M.; Lagerloef, G. S E; Colomb, F.R.; Yueh, S.H.; Pellerano, F.A., "Aquarius: An Instrument to Monitor Sea Surface Salinity From Space," Geoscience and Remote Sensing, IEEE Transactions on , vol.45, no.7, pp.2040,2050, July 2007.

[2] Le Vine, D.M.; Pellerano, F.; Lagerloef, G. S E; Yueh, S.; Colomb, R., "Aquarius: A Mission to Monitor Sea Surface Salinity from Space," IEEE MicroRad, 2006 , vol., no., pp.87,90, 2006.

[3] A. Buis, P. Lynch, G. Cook-Anderson, Ro. Sullivant, "Aquarius/SAC-D: Studying Earth's salty seas from space", Jun. 2011.

[4] Lagerloef, G. S E; Chao, Y.; Colomb, F.R., "Aquarius/SAC-D Ocean Salinity Mission Science Overview," Geoscience and Remote Sensing Symposium, 2006. IGARSS 2006, IEEE International Conference on , vol., no., pp.1675,1677, July 31 2006-Aug. 4 2006.

[5] Biswas, S.K.; Jones, L.; Rocca, D.; Gallio, J.-C., "Aquarius/SAC-D Microwave Radiometer (MWR): Instrument description & brightness temperature calibration," Geoscience and Remote Sensing Symposium (IGARSS), 2012 IEEE International , vol., no., pp.2956,2959, 22-27 July 2012.

[6] Le Vine, D.M.; Lagerloef, G. S E; Pellerano, F.; Colomb, F.R., "The Aquarius/SAC-D mission and status of the Aquarius instrument," Microwave Radiometry and Remote Sensing of the Environment, 2008, MICRORAD 2008, vol., no., pp.1,4, 11-14 March 2008.

[7] Le Vine, D.M.; Lagerloef, G. S E; Torrusio, S.E., "Aquarius and Remote Sensing of Sea Surface Salinity from Space," Proceedings of the IEEE, vol.98, no.5, pp.688,703, May 2010.

[8] Le Vine, D.M.; Lagerloef, G. S E; Torrusio, S., "Aquarius and the Aquarius/SAC-D mission," Microwave Radiometry and Remote Sensing of the Environment (MicroRad), 2010 11th Specialist Meeting on , vol., no., pp.33,36, 1-4 March 2010.

[9] Le Vine, D.M.; Lagerloef, G. S E; Yueh, S.; Pellerano, F.; Dinnat, E.; Wentz, F., "Aquarius Mission Technical Overview," Geoscience and Remote Sensing Symposium, 2006. IGARSS 2006, IEEE International Conference on, vol., no., pp.1678,1680, July 31 2006-Aug. 4 2006.

[10] Le Vine, D.M.; Lagerloef, G. S E; Ruf, C.; Wentz, F.; Yueh, S.; Piepmeier, J.; Lindstrom, E.; Dinnat, E., "Aquarius: The instrument and initial results," Microwave

Radiometry and Remote Sensing of the Environment (MicroRad), 2012 12th Specialist Meeting on , vol., no., pp.1,3, 5-9 March 2012.

[11] Yueh, S.H.; West, R.; Wilson, W.J.; Fuk K.Li; Njoku, E.G.; Rahmat-Samii, Y., "Error sources and feasibility for microwave remote sensing of ocean surface salinity," Geoscience and Remote Sensing, IEEE Transactions on , vol.39, no.5, pp.1049,1060, May 2001.

[12] Shadi Aslebagh, W.Linwood Jones, and Hamideh Ebrahimi, "Negative Impacts of Rainfall on Aquarius Sea Surface Salinity Measurements", Proc. IEEE International Symposium on Antenna and Propagation, Orlando, FL, Jul. 7-13, 2013.

[13] Hamideh Ebrahimi, Shadi Aslebagh, and Linwood Jones, "Use of Monte Carlo Simulation in Remote Sensing Data Analysis", Proc. IEEE SoEastCon, Jacksonville, FL, Apr. 5-7, 2013.

[14] J. C. Gallo, Aquarius/SAC-D Microwave Radiometer Critical Design Review," Buenos Aires, Argentina, August 22-24, 2007.

[15] Hejazin, Y.; Aslebagh, S.; Jones, W.L., "Aquarius/SAC-D MicroWave Radiometer ocean wind speed measurements," Oceans, 2012 , vol., no., pp.1,4, 14-19 Oct. 2012.

[16] Aslebagh, S.; Hejazin, Y.; Jones, W.L.; May, C.; Gonzalez, R., "An oceanic rain flag for Aquarius," Oceans, 2012, vol., no., pp.1,4, 14-19 Oct. 2012.

[17] Bolvin, D.T.; Adler, R.F.; Huffman, G.J.; Nelkin, E.J., "A first comparison of global merged precipitation analyses with Tropical Rainfall Measuring Mission (TRMM) data," Geoscience and Remote Sensing Symposium Proceedings, 1998. IGARSS '98. 1998 IEEE International , vol.4, no., pp.1892,1894 vol.4, 6-10 Jul 1998.

[18] Readme for TRMM product 3B42 (7), Goddard Earth Science Data and Information Services Center, Nov. 2012.

<http://disc.sci.gsfc.nasa.gov/precipitation/documentation/TRMM_README/TRMM_3B42_readme.shtml>

[19] Aquarius Level-2 Data Product Version 1.3.2, NASA Goddard Spaces Flight Center's Aquarius Data Processing System, Jul. 2012.

[20] Aquarius Data Access Link, NASA JPL PO.DAAC, Nov. 2012.

<http://podaac.jpl.nasa.gov/SeaSurfaceSalinity/Aquarius>

[21] G.J. Hoffman, R.F. Adler, M.M. Morrissey, D.T. Bolvin, S. Curtis, R. Joyce, B. McGavock and J. Susskind, "Globa Pricipitation at One-degree daily Resolution from Multisatellite Observation", Journal of Hyderometeorology, Oct 2000.

[22] G.J. Hoffman and D.T. Bolvin, “TRMM and Other Data Precipitation Data Set Documentation”, Mesoscale Atmospheric Process Laboratory, NASA Goddard Space Flight Center and Science Systems and Applications, Jan 2013.

[23] Bidwell, S.W. Flaming, G.M. Durning, J.F. Smith, E.A., "The Global Precipitation Measurement (GPM) Microwave Imager (GMI) instrument: role, performance, and status," Geoscience and Remote Sensing Symposium, 2005. IGARSS '05. Proceedings. 2005 IEEE International, vol.1, no., pp. 4 pp., 25-29 July 2005.

[24] TRMM 3B42 Data Access Link, NASA, Goddard Earth Science Data and Information Service Center, Nov. 2012.

<http://mirador.gsfc.nasa.gov/cgi-bin/mirador/presentNavigation.pl?tree=project&dataset=3B42:%203-Hour%200.25%20x%200.25%20degree%20merged%20TRMM%20and%20other%20satellite%20estimates&project=TRMM&dataGroup=Gridded&version=007>

[25] G.J. Huffman, R.F. Adler, D.T. Bolvin, G. Gu, E.J. Nelkin, K.P. Bowman, Y. Hong, F.F. Stocker and D.B. Wolf, "The TRMM Multisatelite precipitation Analysis (TMPA)", Jouranl of hydrometeorolgy, vol. 8, June 2006.

[26] Teng Hongfen; Tian Yanfeng; Shi Zhou; Jin Huiming, "Spatial-temporal accuracy validation and uncertainty analysis for TRMM 3B42 data at provincial scale in China," Agro-Geoinformatics (Agro-Geoinformatics), 2012 First International Conference on , vol., no., pp.1,4, 2-4 Aug. 2012.

[27] Zheng Duan; Bastiaanssen, W. G M; Junzhi Liu, "Monthly and annual validation of TRMM Mulitisatellite Precipitation Analysis (TMPA) products in the Caspian Sea Region for the period 1999–2003," Geoscience and Remote Sensing Symposium (IGARSS), 2012 IEEE International , vol., no., pp.3696,3699, 22-27 July 2012.

[28] Gaiser, P.W.; St Germain, K.M.; Twarog, E.M.; Poe, G.A.; Purdy, W.; Richardson, D.; Grossman, W.; Jones, W.L.; Spencer, D.; Golba, G.; Cleveland, J.; Choy, L.; Bevilacqua, R.M.; Chang, P.S., "The WindSat spaceborne polarimetric microwave radiometer: sensor description and early orbit performance," Geoscience and Remote Sensing, IEEE Transactions on , vol.42, no.11, pp.2347,2361, Nov. 2004.

[29] Joyce, Robert J., John E. Janowiak, Phillip A. Arkin, Pingping Xie, "Cmorph: a method that produces global precipitation estimates from passive microwave and infrared data at high spatial and temporal resolution.", J. Hydrometeor, 2004: 5, 487–503.